

Review

# Surface Treatment of Biochar—Methods, Surface Analysis and Potential Applications: A Comprehensive Review

Marlena Geça <sup>1</sup>, Ahmed M. Khalil <sup>2,3,\*</sup>, Mengqi Tang <sup>3</sup>, Arvind K. Bhakta <sup>3,4</sup>, Youssef Snoussi <sup>3</sup>, Piotr Nowicki <sup>5</sup>, Małgorzata Wiśniewska <sup>1,\*</sup> and Mohamed M. Chehimi <sup>3,\*</sup>

<sup>1</sup> Department of Radiochemistry and Environmental Chemistry, Institute of Chemical Sciences, Faculty of Chemistry, Maria Curie-Skłodowska University in Lublin, M. Curie-Skłodowska Sq. 3, 20-031 Lublin, Poland; marlena.geca@wp.pl

<sup>2</sup> Photochemistry Department, National Research Centre, Dokki, Giza 12622, Egypt

<sup>3</sup> ITODYS (UMR 7086), CNRS, Université Paris Cité, 75013 Paris, France; meng7tang@outlook.com (M.T.); arvind-kumar.bhakta@u-paris.fr (A.K.B.); youssef.snoussi@u-paris.fr (Y.S.)

<sup>4</sup> Department of Chemistry, St. Joseph's University (Autonomous), Bangalore 560027, India

<sup>5</sup> Department of Applied Chemistry, Faculty of Chemistry, Adam Mickiewicz University in Poznań, Uniwersytetu Poznańskiego 8, 61-614 Poznań, Poland; piotr.nowicki@amu.edu.pl

\* Correspondence: akhalil75@yahoo.com (A.M.K.); malgorzata.wisniewska@mail.umcs.pl (M.W.); mohamed.chehimi@cnrs.fr (M.M.C.)

**Abstract:** In recent years, biochar has emerged as a remarkable biosourced material for addressing global environmental, agricultural, biomedical, and energy challenges. However, the performances of biochar rest in part on finely tuning its surface chemical properties, intended to obtain specific functionalities. In this review, we tackle the surface treatment of biochar with silane and other coupling agents such as diazonium salts, titanates, ionic/non-ionic surfactants, as well as nitrogen-containing (macro)molecules. We summarize the recent progress achieved mostly in the last five years and correlate the nature and extent of functionalization to eye-catching end applications of the surface-engineered biochar.

**Keywords:** biomass conversion; thermochemical treatment; surface chemical modification; coupling agents; biochar implementation



**Citation:** Geça, M.; Khalil, A.M.; Tang, M.; Bhakta, A.K.; Snoussi, Y.; Nowicki, P.; Wiśniewska, M.; Chehimi, M.M. Surface Treatment of Biochar—Methods, Surface Analysis and Potential Applications: A Comprehensive Review. *Surfaces* **2023**, *6*, 179–213. <https://doi.org/10.3390/surfaces6020013>

Academic Editor: Gaetano Granozzi

Received: 18 March 2023

Revised: 26 May 2023

Accepted: 28 May 2023

Published: 2 June 2023



**Copyright:** © 2023 by the authors. Licensee MDPI, Basel, Switzerland. This article is an open access article distributed under the terms and conditions of the Creative Commons Attribution (CC BY) license (<https://creativecommons.org/licenses/by/4.0/>).

## 1. Introduction and Scope of the Review

It is without any doubt that biochar is a very hot topic due to its central position at the crossroads of materials science, materials and surface chemistry, surface science, catalysis, and organic reactions. Biochar is at the heart of sustainable development and concerns biomass and waste valorization and utilization for de-pollution and soil amendment. Such an infatuation for biochar is motivated by the availability of numerous varieties of biomasses and wastes worldwide and the need for valorization and/or transformation into functional materials. This resulted in skyrocketing number of publications, exceeding 5500 since 2021.

The most important applications of biochar concern soil amendment and agriculture [1–3], but recently much has been achieved in the design of biochar-supported nanocatalysts for water treatment consisting of total mineralization of organic pollutants such as dyes and drugs [4,5], or for the reductive process [6], or for catalyzing organic chemistry reactions [7,8]. Other applications concern the use of biochar as fillers in composite materials [9–11], electrode materials [12,13], and the development of novel engineered biochar for the treatment of neglected tropical diseases (NTDs) [14,15], to name just these applications.

Whilst biochar can be employed as freshly obtained by thermochemical conversion of the biomass, it nevertheless requires particular surface treatment in order to impart it with new functionalities. In this mini-review, the focus is on the functionalization of biochar with molecular/macromolecular surface modifiers or coupling agents and catalytic

nanoparticles, regardless of any pretreatment of the biomass or post-treatment of the biochar, or conducting pyrolysis under various gases such as  $N_2$ ,  $N_2/H_2$  [16], or  $CO_2$  [8],  $NH_3$ , etc. For more details about specific activation strategies of biochar, the reader is referred to the shortlisted reviews gathered in Table 1.

**Table 1.** Shortlisted, relevant reviews tackling applications of surface-engineered biochar.

Running Title	Review Main Topic	Year Review Published	References
Biochar for catalytic biorefinery and environmental processes	The article summarizes the knowledge on the production of biochar, its classical activation with aggressive compounds, and its use to expedite biorefinery operations and degradation of environmental pollutants	2019	[17]
Chemically modified carbonaceous adsorbents for $CO_2$ capture	The review discusses activation, surface amination or carboxylation, and doping of various carbon allotropes, including biochar, for extensive capture of $CO_2$ .	2021	[18]
Biochar as a support for nanocatalysts and other reagents	The review paper summarizes the knowledge on the use of biochar-supported nanocatalyst, and discusses the mode of coordination of the catalyst nanoparticles by the biochar.	2021	[19]
Phosphorus adsorption by functionalized biochar	Inefficient crop fertilization induces water pollution by phosphorus. The review discusses biomass pretreatment as well as post-modification of biochar to obtain efficient phosphorus porous adsorbents	2022	[20]
Surface modification of biochar for dye removal	The review discusses several strategies of obtaining functional biochar for the removal of dyes from water.	2022	[21]
Biochar for the removal of contaminants from industrial wastewaters	The paper reviews methods for obtaining pristine and engineered biochar for the efficient removal of numerous contaminants from industrial wastewaters.	2022	[22]
Biochar as a reinforcing bio-based filler in rubber composites.	This article is focused on the key properties of highly reinforcing fillers, such as particle size, structure, and surface activity. The review essentially covers silane modification of biochar.	2023	[10]

These reviews concerned various carbon allotrope surface modifications [18], classical activation methods [17] that rest on acid or alkali treatment of biochar, activation with metal chlorides, and post-pyrolysis under steam, to name but a few. However, despite the numerous advances in biochar production, post-modification, and applications, only a few reviews covered surface modification, for example, the surface treatment of biochar particles with silanes for the design of high performance composites (see Table 1). Coverage of the chemical modification of biochar surface with a large series of well-known coupling agents such as silanes, diazonium salts, aminated compounds, surfactants and macromolecules is lacking despite its interest in several domains, i.e., organic chemistry, polymer science and technology, environmental remediation, and sustainable energy. This is what has motivated this review article.

## 2. Biomass Conversion to Biochar

Biochar and other related porous carbon materials can be obtained by conversion of biomass using pyrolysis under an inert or reducing atmosphere. Figure 1 displays the impact of pyrolysis parameters on the types of products obtained [23–26]. Slow pyrolysis is the recommended technique for obtaining biochar.

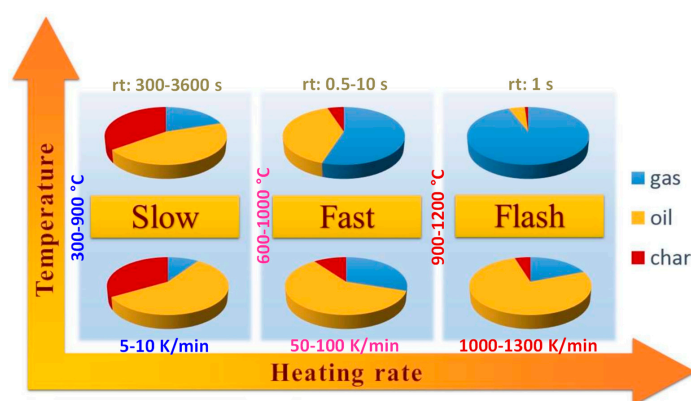


**Figure 1.** Pyrolysis techniques and the effect of process parameters on product distribution (*rt*: residence time). Adapted from [26].

Carbonization could also be achieved through different processes, namely hydrothermal treatment to produce hydrochar [27], microwave-assisted carbonization [28], laser-induced biochar elaboration [29], gasification [30], and torrefaction [31].

The biochar-making method governs its textural and structural properties and chemical composition. These characteristics decide the potential application of the carbonaceous matter. For example, microwave pyrolysis is recommended for applications such as adsorption and heterogeneous catalysis; indeed, the latter requires a pronounced porous structure and a high specific surface area. Moreover, an increased yield of high-quality biochar could be obtained by microwave pyrolysis compared to the conventional pathways [32]. Gasification based on partial oxidation of the bio-feedstock using carbon dioxide, oxygen, air, steam, or a mixture of these gases, promotes the production of syngas/producer gas, resulting in a relatively low biochar yield in the 5–10 percentage range [33]. The pyrolysis conditions (temperature, residence time) of biomass are known to be the key factor controlling the polycyclic aromatic hydrocarbons (PAHs) and volatile organic compounds (VOCs) content in biochar; their control is crucial to monitor the release of PAHs and VOCs from the carbonized biomass in soil amendment application [34,35].

Besides the conversion method, the initial biomass could be mixed with  $ZnCl_2$  or  $KOH$ , or  $H_3PO_4$  (used before or after pyrolysis) in order to control the biochar yield and textural properties [23]. As noted above, the gas used during pyrolysis has a major effect on the chemical structure. For example, the mixture  $N_2/H_2$  induces less oxygen in the final biochar and a higher isoelectric point (IEP) compared to the same biochar obtained using pure  $N_2$  [16]. Textural properties could be controlled via green approaches consisting of mechanical grinding [36] or maceration of the initial biomass in a water/alcohol mixture [15]. We have recently noted that the preparation of biochar@nickel composite by pyrolysis of biomass impregnated with nickel salt-induced an unusual fishnet-like structure of biochar [37]. Actually, nickel catalyzes the carbonization of biomass and leads to a more porous biochar structure [38].

### 3. Biochar Surface Treatment Pathways

#### 3.1. General Aspects

Figure 2 schematically illustrates shortlisted pathways for chemical modification of biochar surface. The literature survey using Google Scholar and the Web of Science indicated that the most employed compounds are silane coupling agents, ionic or non-ionic surfactants, and aryl diazonium salts. For catalytic purposes, titanates have also been proposed. Silanes require hydroxylated surfaces and thus are applicable to biochar as most biochar materials are prepared by thermochemical conversion at 300–500 °C, a range of temperature that ensures the presence of reactive functional groups such as OH and C=O [21]. Such groups can also be obtained by post-acidic treatment [21,39]. Concerning diazonium salts, most carbon allotropes react with these modern surface modifiers to provide C-C bonds and ester linkages [40]. As far as surfactants are concerned, anionic and cationic surfactants interact with biochar via completely different mechanisms (biochar-hydrophobic tail, or biochar-hydrophilic head) [41]. Non-ionic surfactants have completely different behavior and rather interact with biochar via oxygen atoms or OH groups (see Section 3.4). Titanates are able to form  $TiO_2$  nanoparticles, in situ, at the surface of biochar and are thus important for providing photocatalytic composites [42]. Another emerging coupling agent is polyethyleneimine (PEI) [43].

In this review, we concentrate on coupling agents that react/interact chemically with biochar, via covalent linkages or through strong electrostatic interactions, hydrogen bonds, or hydrophobic interactions. Other strategies consisting of direct immobilization of nanocatalysts on biochar obtained by pyrolysis of biomass impregnated with metal salt precursor will be briefly summarized at the end of the review.

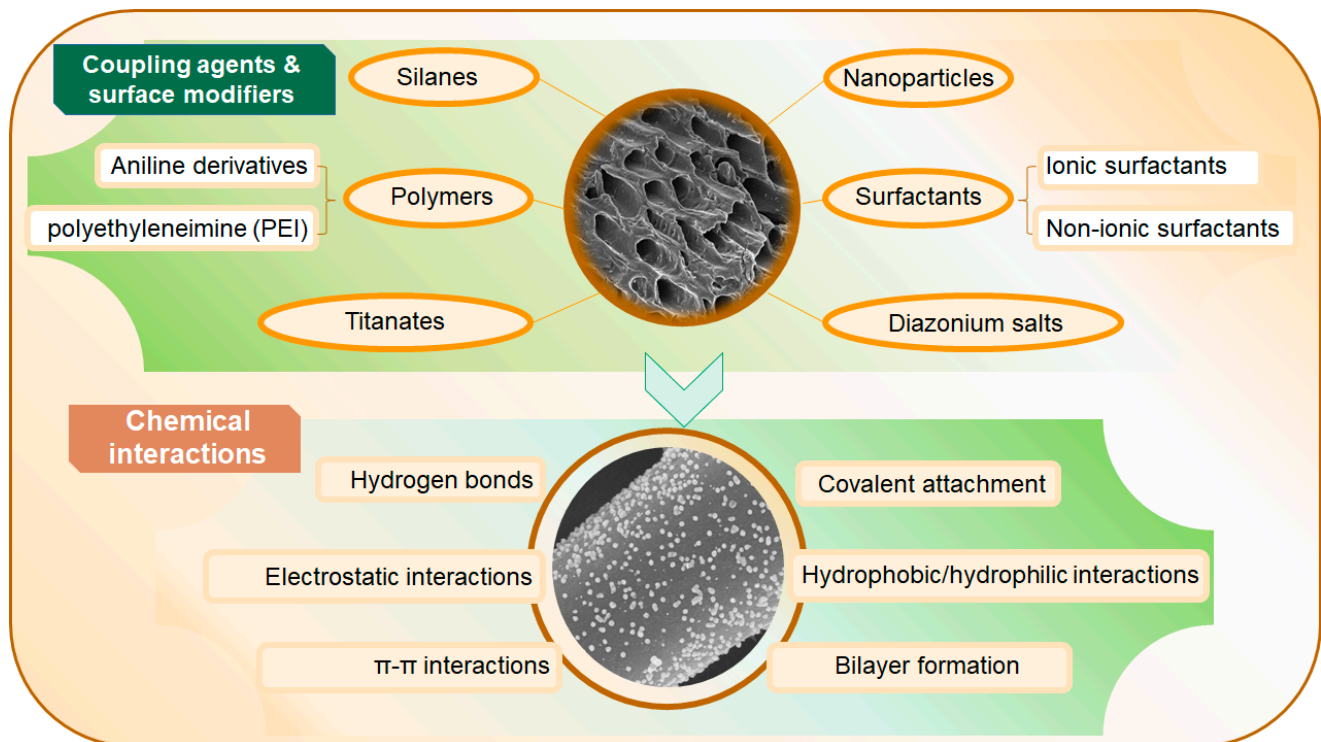


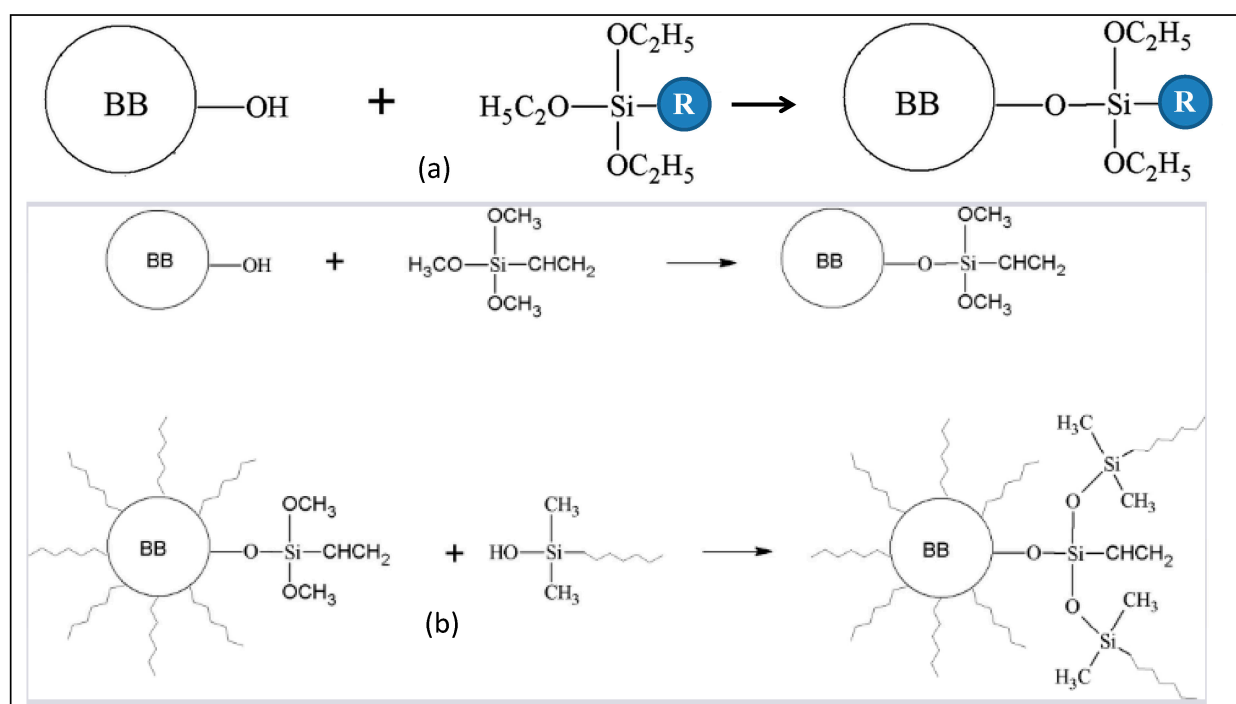
**Figure 2.** Schematic illustration of biochar surface treatment with popular coupling agents.

### 3.2. Surface Functionalization with Silane Coupling Agents

Silanization is the process of modification of surfaces by incorporating organofunctional alkoxy silane [44]. The reaction is usually conducted in aqueous or hydro-alcoholic media. The important steps in silanization are [45]: (i) silane hydrolysis, which leads to  $R-Si(OH)_3$ , (ii) hydrogen bonding between the hydrolyzed silane and the surface, (iii) condensation with the surface resulting in surface-O-Si linkage, (iv) possible polymerization of the silane in solution, and (v) reaction with pending R group with other species as is briefly discussed below.

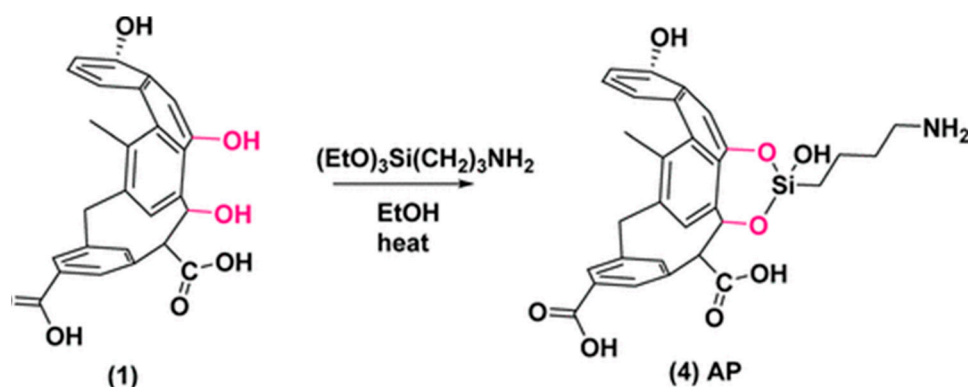
In the case of biochar, the abundance of -OH functional groups is crucial for its functionalization with silane coupling agents. Such a modification permits the fabrication of high-performance biochar-filled polymer composites, immobilized catalysts, and metal complexes, materials for electromagnetic shielding and road engineering, among numerous applications. We will select a few case studies of distinct types of applications in order to show the possibilities offered by silanes to impart new functionalities and performances to biochar.

Figure 3a depicts a general pathway of functionalization of biochar that bears surface hydroxyl groups. The group R borne by the silane is chosen in a way it imparts a specific functionality to biochar: post-functionalization, hydrophilic/hydrophobic interactions, metal complexation/chelation, in situ polymerization, and dispersion in the polymer matrix. Indeed, modified biochar can be used to make composite membranes for pervaporation, a process that uses a poly(dimethyl siloxane) (PDMS) for the separation of ethanol/water mixture [46]. Figure 3b shows the steps involved in biochar silanization. Firstly, silanes go through hydrolysis, followed by condensation, to produce oligomers. Finally, oligomers react with -OH groups on the biochar surface, thus leading to biochar-O-Si covalent bonds [47]. Pending methoxy groups react with PDMS, which results in a biochar/PDMS composite membrane. Vinyl-silanized biochar imparts superior hydrophobic properties to the PDMA membrane compared to aminosilane, as the latter interacts favorably with water due to its free amine group [46].



**Figure 3.** (a). General pathway for the silanization of biochar. R =  $-(\text{CH}_2)_3\text{NH}_2$ ,  $-(\text{CH}_2)_3\text{Cl}$ ,  $-(\text{CH}_2)_3\text{SH}$ ,  $-(\text{CH}_2)_3\text{O}-(\text{C}=\text{O})-(\text{C}=\text{CH}_2)\text{CH}_3$ ,  $-\text{CH}=\text{CH}_2$ . . . . (b) Silanization of wood biochar with vinylsilane, followed by reaction with PDMS. Reproduced from [46] with permission of John Wiley & Sons.

Silanization of the surface with monosilane (Figure 4), followed by condensation, led to a removal capacity of  $\text{CO}_2$  3.7 mmol/g (specific surface area SSA = 394  $\text{m}^2/\text{g}$ ), higher than 3.4 mmol/g, obtained with Norit, a commercial product of which SSA = 3.4 mmol/g [48].



**Figure 4.** Modification of biochar surface with aminosilane coupling agent. Reproduced from [48] with permission of ACS.

Silanization could be an important step to enable the post-functionalization of biochar with complex structures such as metal chelators. Figure 5 depicts a strategy for anchoring ruthenium (Figure 5a), iron, and nickel-containing moieties (Figure 5b). They have exhibited enhanced catalytic activity with high turnover frequency for organic reactions.

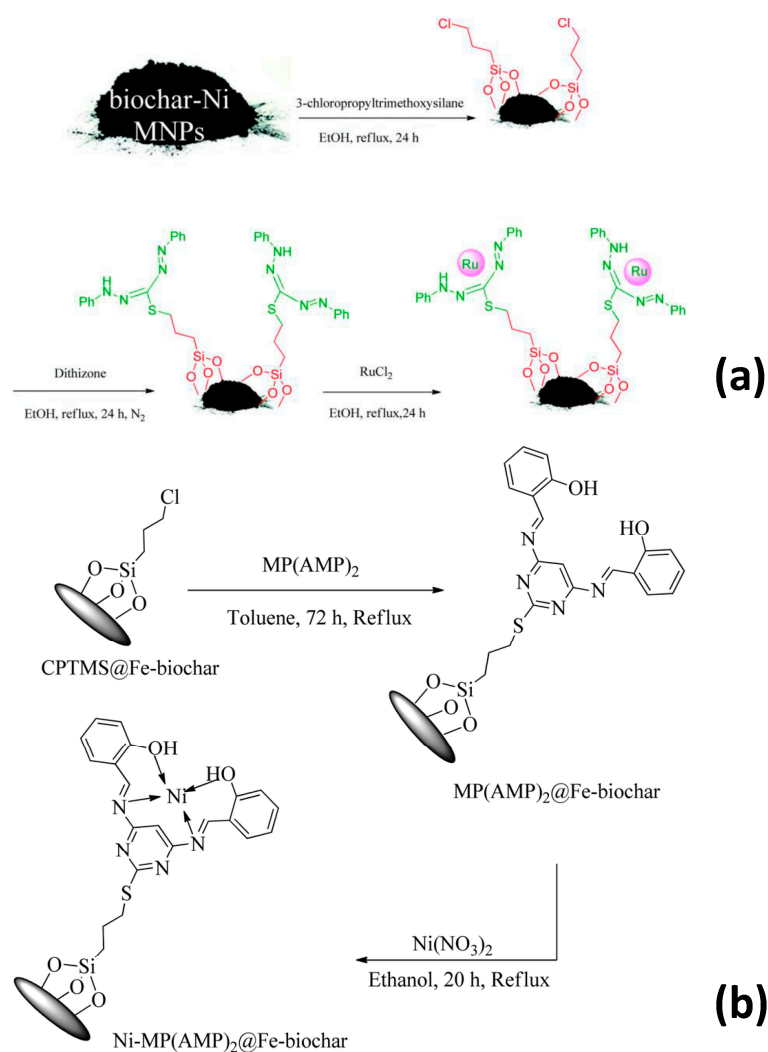


**Figure 5.** Strategies to design silanized biochar for the immobilization of heterogeneous catalysts of organic chemical reactions: Biochar@Ni modified with silane for covalent coupling of ruthenium ligand (a), and chloro-silanized biochar, post-modified with mercaptan derivative for chelating nickel catalyst (b). (a) Reproduced with permission of RSC, from [49] (a), and from [50] (b).

If silanization permits to impart of new functionality to biochar, the spatial distribution of the surface-bound reactive groups is an issue. For example, Huang et al. [51] have brought strong supporting evidence for the effect of pyrolysis temperature on the silanization extent of pine sawdust biochar; they have shown that mercapto-silanization was more efficient with the decreasing order of temperature  $300 > 500 > 700$  °C. Indeed, biochar has much more OH, C=O, and COOH groups at low pyrolysis temperatures, therefore, enabling even distribution of SH groups at the surface, resulting in larger removal of Hg(II) and  ${}^3\text{HCHg}^+$  ions (Figure 6). Interestingly, the high-resolution S2p region from 3BS biochar (prepared at 300 °C and silanized) exhibited peak broadening due to the formation of mercury sulfide. Although 3B and 3BS samples exhibited the lowest specific surface area (1.7 and 4.2  $\text{m}^2/\text{g}$ , respectively), substantial mercury compounds could be removed (see Figure 6b,c). This is a clear indication that an even and densely packed distribution of mercapto groups overcame the textural properties imparted by high pyrolysis temperature (335 and 235  $\text{m}^2/\text{g}$  for 7B and 7BS, respectively).

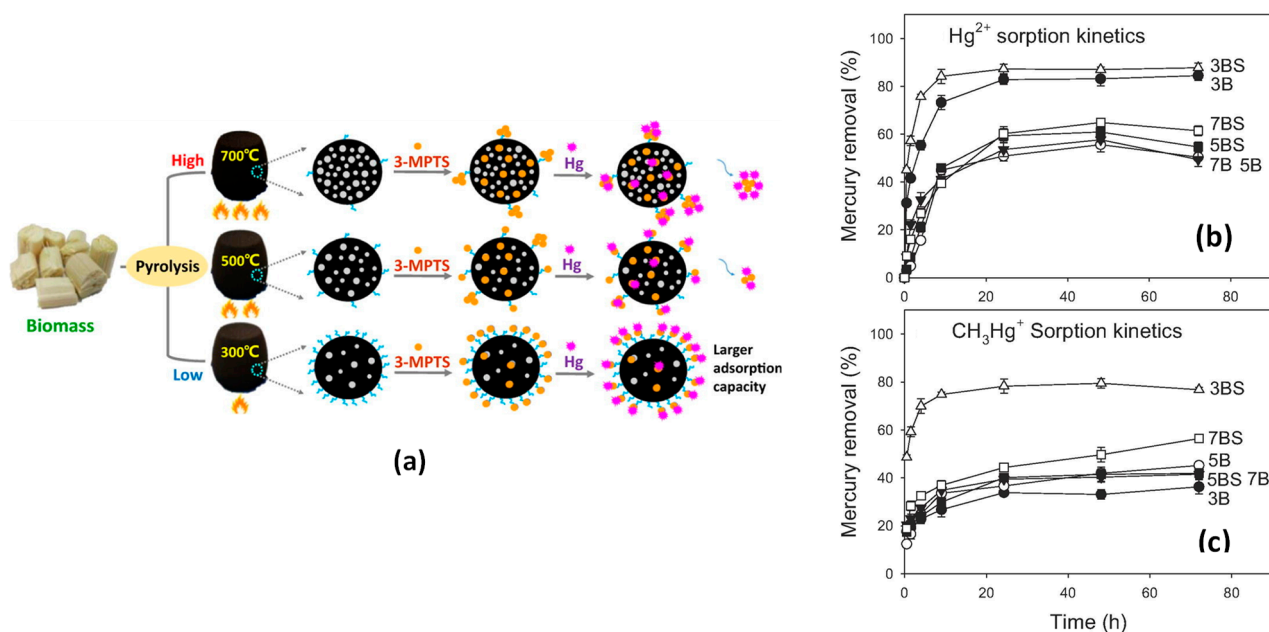


**Figure 6.** Fabrication of mercapto-silanzed biochar for the removal of Hg compounds. Schematic illustration of the pyrolysis temperature effect on silanization extent, textural and adsorption capacity of biochar (a); effect of pyrolysis temperature and silanization on the removal of  $Hg^{2+}$  (b), and  $CH_3Hg^+$  (c). Reproduced from [51] with permission of Elsevier.

Table 2 reports different silane coupling agents employed to modify biochar surfaces and their potential applications. It shows that either silane-modified biochar or their further modification has been used for different purposes, including water treatment, nanoparticles capture, polymer reinforcement, membranes, road engineering, landfill cover, etc.

**Table 2.** Surface treatment of biochar with silane coupling agents.

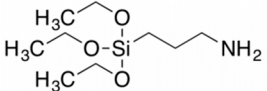
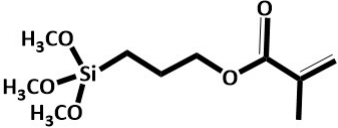
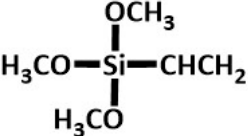
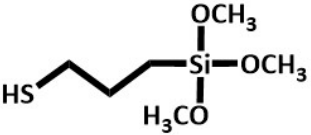
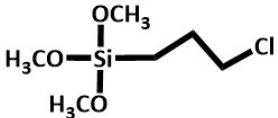
Coupling Agent	Biomass	Surface Treatment Conditions	Properties of Engineered Biochar	Potential Application	Refs.
 APTES	Sawmill residues	Char/water = 10/1; 2 wt.% APTES; condensation at pH 3–4 for 1 h followed by reaction at 70 °C for 6 h. Post-activation in air at 560 °C.	SSA = 394 m <sup>2</sup> /g; 0.24 wt.% N;	CO <sub>2</sub> adsorption capacity of 3.7 mmol/g	[48]
	Oil sludge	C <sub>2</sub> H <sub>5</sub> OH: H <sub>2</sub> O: KH-550 ratio of 70: 25: 5, left for 60 min. Then, oil sludge pyrolysis residue added and stirred for 1 h, followed by drying at 60 °C. (KH-550: aminosilane)	Rheological properties (rutting resistance factor, creep stiffness, and high-temperature performance) improvement of the asphalt mortar	Road engineering	[52]
	Onion peels	Silane (3 wt.%) was mixed with C <sub>2</sub> H <sub>5</sub> OH- H <sub>2</sub> O solution (95 wt% C <sub>2</sub> H <sub>5</sub> OH + water + acid 5%), stirred for 10 at room temp. Then, ball-milled Co-biochar was incorporated, rinsed for 10 min and filtered, and finally dried at 110 °C.	High tensile strength and EMI: −44.37 dB and −49.62 dB for X and Ku band	PVA composite For EMI application	[53]
KH-570 	Rice straw	Mixture of pre-treated biochar + 20% (v/v) KH-570, 72% (v/v) absolute C <sub>2</sub> H <sub>5</sub> OH + 8% (v/v) H <sub>2</sub> O, magnetically stirred at 30 °C, mixed with modifier for 12 h, washed with ethanol, filtered and dried at 50 °C.	Enhanced CH <sub>4</sub> oxidation	Soil cover for landfill gas control.	[54]
	Rice straw	-	H <sub>2</sub> O absorption = 1.27 g (g biochar) <sup>-1</sup> Water proofing, MOB growth promotion, ventilation and efficient CH <sub>4</sub> reduction.	Landfill cover soil	[55]
YDH-171 	lodgepole pine bark	Synthesized biochar at 600 °C and modified by YDH-171. Further, 3 wt.% modified were taken for further experiment	PV performance: separation factor (11.3) and flux (227.25 g m <sup>-2</sup> h <sup>-1</sup> ).	PV membranes (Separating C <sub>2</sub> H <sub>5</sub> OH from H <sub>2</sub> O.	[46]
A-189 	Bamboo	Pre-treated ultrafine bamboo char was mixed with A-189 (16 w/w%). Following silane treatment, oven-dried for 24 at 105 °C.	Tensile strength (18.87 MPa) and tensile modulus (272 MPa) increased by 99.3% and 104.9%.	Polymer reinforcement	[56]

Table 2. Cont.

Coupling Agent	Biomass	Surface Treatment Conditions	Properties of Engineered Biochar	Potential Application	Refs.
CPTMS 	Chicken manure	<p>Pyrolyzed biomass (400–800 °C, 1 to 2 h) was treated with CPTMS followed by dispersion in 1.5 mmol TBA and toluene and stirred for 48 h at 90 °C. Residue was isolated, washed with C<sub>2</sub>H<sub>5</sub>OH, and dried (50 °C). Then, Pd (OAc) and NaBH<sub>4</sub> treatment at optimum condition.</p>	<p>In the synthesis of biphenyl derivatives (yield = 97%, TON = 135, and TOF = 405)</p>	<p>C-C coupling reaction (Suzuki–Miyaura and Heck–Mizoroki cross-coupling reactions.)</p>	[57]
		<p>Biochar-Ni magnetic composite was refluxed with 1.5 silane in the presence of EtOH for 24 h. Several other steps followed by treatment with dithizone and RuCl<sub>2</sub> lead to formation of Ru-dithizone@biochar-Ni MNPs</p>	<p>High catalytic activity for C-C coupling reaction of iodobenzene or chlorobenzene with 96% yield.</p>	<p>Suzuki C-C coupling reaction</p>	[49]
		<p>CPTMS@Fe-biochar was treated with MP(AMP)<sub>2</sub> and refluxed for 72 h in the presence of toluene, and then the product is refluxed with ethanol and nickel nitrate for 20 h.</p>	<p>Enhanced catalytic efficiency. Catalyst recovery through a magnet. Homoselectivity was observed. %yield = 98%. Recyclable up to 9 times.</p>	<p>Catalysis (synthesis of tetrazole derivatives)</p>	[50]

APTES: aminopropyl triethoxysilane; EMI: electromagnetic interference shielding; PV: Pervaporation; PVA: Poly vinyl alcohol; SSA: specific surface area; TOF: turnover frequency.

### 3.3. Titanate Surface Modifiers

Titanates are well-known coupling agents in composite science and technology [58,59], generally speaking, and more specifically, in the domain of dental materials [60,61]. They are proposed for the fabrication of robust dental composite materials.

They have been explored in surface modification of rice bran biochar, but without mention of potentially occurring surface reaction [42]. For this purpose, magnetic biochar was prepared by post-modification with Fe(II) and Fe(III) iron chlorides via pyrolysis, followed by sol-gel process synthesis of TiO<sub>2</sub> from titanate in the presence of the magnetic biochar@Fe. The final material was applied for the photocatalyzed removal of tetracycline antibiotics and for antibacterial application. Of particular interest to surface and interface phenomena, Ti-O-C interfacial functional group was probed by FTIR, which accounts for the covalent attachment of TiO<sub>2</sub> to the underlying biochar.

In another study, titanates were used in order to modify preformed biochar in a sol-gel process. The titanate-modified biochar was pyrolyzed in order to obtain biochar@TiO<sub>2</sub>. Further, wetting impregnation with silver nitrate followed by pyrolysis resulted in biochar@TiO<sub>2</sub>-Ag with antibacterial activity against *E. coli* (99% of sterilization ratio in 5 min, under daylight) [62].

XPS analysis was used to probe titanate interaction with carbon allotropes, but only rare examples have been found. For example, activated carbon was treated with titanate in order to design supercapacitors (specific capacitance: 376.2 F.g<sup>-1</sup>, internal resistance: 0.91 Ω) [63].

Although not strictly on biochar, but of relevance to this review and the scope of the journal *Surfaces*, recently, titanates were proposed for the covalent attachment of graphene oxide (Figure 7) in order to provide surface-bound alkyl groups that ensure dispersion of GO in hydraulic oils [64]. Interestingly, C1s spectra show a drastic decrease in the C-O component due to the covalent attachment of the long alkyl chains to the GO via titanium. Such surface-bound groups permitted excellent dispersion of titanate-modified GO in hydraulic oil with remarkably improved tribological properties.

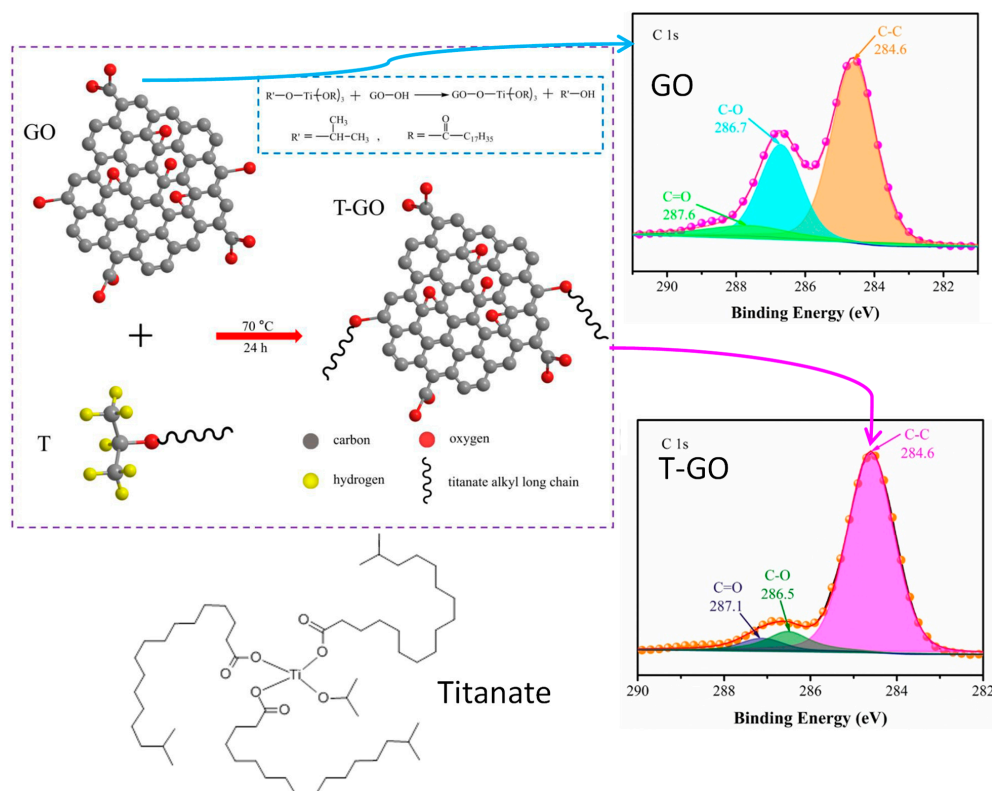


**Figure 7.** Covalent modification of graphene oxide with isopropyl triisostearyl titanate. Reproduced from [64] with permission of Elsevier.

### 3.4. Modification of Biochar by Ionic and Nonionic Surfactants

Biochar surface properties could be changed through modification with the surfactant layers. The ionic and non-ionic surfactant adsorbed on the solid surface influence the specific surface area, the content of acidic–basic functional groups, and the hydrophobic properties of these materials. Various mechanisms of surfactant molecule binding can be involved in such kinds of systems. The electrostatic interactions, hydrogen bonds, interactions between the  $\pi$ - $\pi$  electrons, bilayer formation, and hydrophobic interactions are associated with the adsorption of the surfactant, schematically presented in Figure 8.

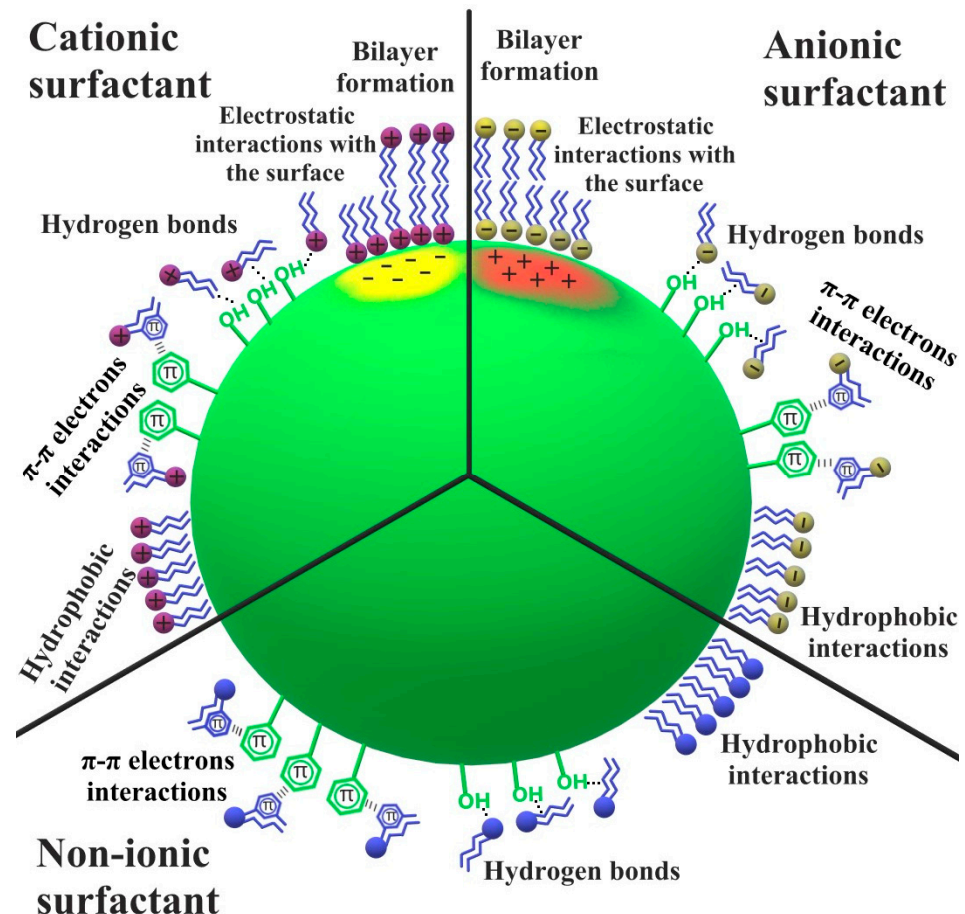


**Figure 8.** Possible adsorption mechanisms of surfactants with various ionic character on biochar surface.

These modifications with the surface active agents can both increase and decrease the biochar adsorption capacity, depending on the adsorbate and surfactant chemical character. The adsorption phenomenon could take place due to all the above-mentioned mechanisms. Moreover, the surfactant-adsorbate multilayer creation and the formation of the micelles have a positive effect on the adsorbed amounts of inorganic and organic substances (Figure 9).

Biochar obtained from the *Populus alba* tree was modified with the cationic surfactant cetyltrimethyl ammonium bromide (CTAB) and used for Cr(VI) adsorption. The obtained results proved that the surfactant modification affects the Cr(VI) adsorption favorably. The adsorbed amount increases on the modified biochar surface in comparison with the non-modified one, independently of the adsorbent dose [65]. CTAB was also used for the biochar derived from the rice husk. The obtained results showed that due to the modification of the adsorbent, its surface charge changed to be positive. The modified biochar was used for inorganic nitrogen fertilizers removal from the aqueous solution. The

removal percentage increased by 13% in the case of the modified adsorbent application in comparison to the non-modified material [66].

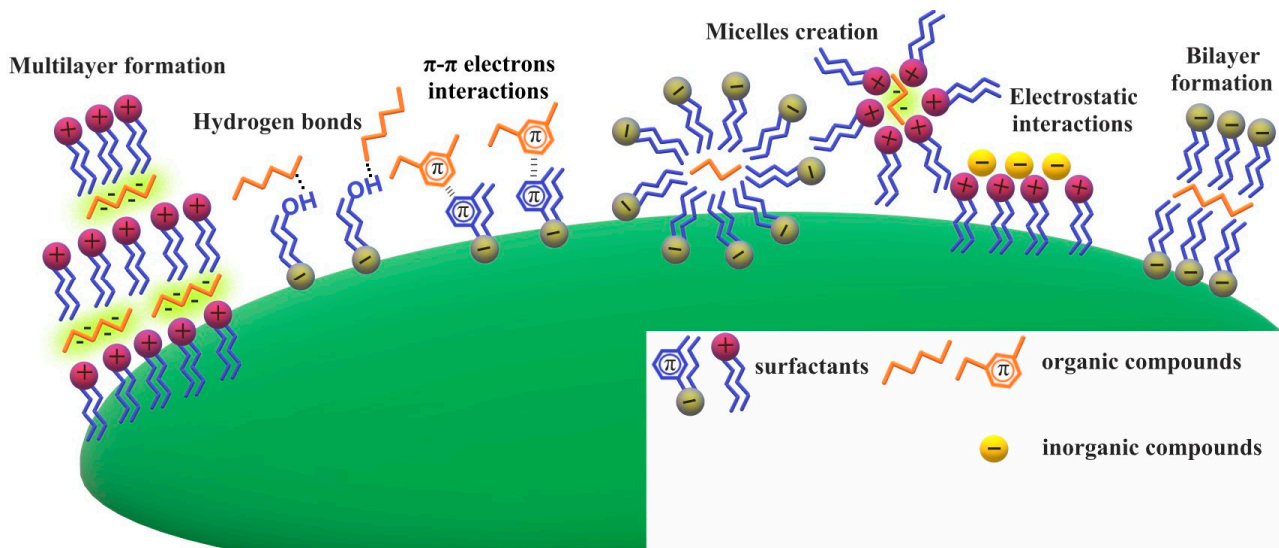


**Figure 9.** Possible mechanisms of organic and inorganic compounds adsorption on surfactant-modified biochar surface.

The cationic CTAB modification was also performed in the case of the activated biochars obtained from the peanut shells and corncobs used for the anionic polymer-poly(acrylic acid) (PAA) adsorption. The surfactant modification favored the increase in the polymer adsorption amount on both examined adsorbents. The poly(acrylic acid) removal from the aqueous solution is strongly related to its pH value; however, at all examined pH values (3, 6, 9), the anionic polymer is better adsorbed on the surface of the CTAB-modified activated biochar. In such a case, the maximum PAA adsorbed amount was 68 mg/g [67].

The CTAB-modified biochar obtained from the peanut shells and corncobs was likewise used for the Bisphenol A adsorption. The pyrolysis was performed at 300, 500, and 700 °C. It was found that the CTAB modification inhibits the Bisphenol A adsorption, and this effect becomes stronger with an increasing pyrolysis temperature. It was also proved that when the surfactant concentration applied was higher, a smaller adsorbed amount of Bisphenol was found [68].

The CTAB-modified coffee husk-activated biochar was used for the reactive dye removal from the aqueous solution. The reactive yellow 145 (RDY145) dye adsorbed amount was the largest on the surface of the CTAB-modified activated biochar in comparison to two commercially available different non-modified activated carbons. The pH value has no significant effect on the RDY145 adsorbed amount. The Reactive Red 195 and Reactive Blue 222 dyes were also effectively separated from the aqueous system [69]. The other studies deal with the adsorption of Orange II (OII) and Methylene Blue (MB) dyes on the CTAB-modified biochar obtained from the cornstalk. Due to the adsorbent charge changing to positive (the non-modified biochar has a negative surface charge), the adsorbed amount of positively charged methylene blue decreases. In turn, the adsorbed amount of negatively charged OII increases compared to that observed for non-modified biochar. These effects are related to the electrostatic adsorption mechanism. The obtained maximum removal using the modified biochar was 40% for methylene blue and 100% for OII [70].

The anionic surfactant, sodium dodecyl benzene sulfonate (SDBS), was used for the surface modification of the biochar obtained from the rice husk. The modified adsorbent was used for the inorganic nitrogen fertilizers removal from the aqueous solution. It was proved that the surfactant modification increases the removal efficiency by 2% compared to the non-modified biochar [66].

Sodium dodecyl sulfate (SDS) is an anionic surfactant that was used for the modification of activated biochars obtained from peanut shells, corncobs, and peat. All the above-mentioned adsorbents were used for the poly(acrylic acid) adsorption. The experiments indicated that the SDS modification effect on the PAA adsorbed amount depends largely on the adsorbent type and the solution pH value. On the surface of the activated biochars obtained from the peanut shells and corncobs, poly(acrylic acid) adsorption was inhibited at pH 9; however, at pH 3 and 6, the surfactant modification affected the polymer adsorbed amount favorably. This is probably related to the PAA conformation change at different pH values. The maximum removal was 60% [67]. Moreover, the SDS modification largely reduced the PAA adsorbed amount at pH 4.5, 6, and 9 on the surface of activated biochar derived from the peat compared to the non-modified one. However, at pH 3, the modification did not significantly affect the polymer removal, which remained in the amount of over 90% [71].

The anionic SDBS surfactant was used for the modification of the biochar derived from the peanut shells. The obtained biochar was used for the Bisphenol A adsorption. It was proved that the SDBS modification affects the Bisphenol A adsorbed amount negatively. The inhibition became stronger and stronger with the increasing surfactant concentration. The Bisphenol A amount adsorbed on the surface of the non-modified biochar was 100 mg/g, and on the surface of SDBD-modified biochar was 10 mg/g [68].

The biochar obtained from the cassava peels was modified with the SDBS and SDS surfactants and used for Methylene Blue adsorption. It was proved that the SDBS-modified sample resulted in a larger number of surface active sites and increased the dye adsorbed amount. In the case of SDS, due to the changes of the adsorbent surface charge to negative, it had a favorable impact on the dye adsorbed amount increase [72,73]. MB was also adsorbed on the surface of the SDS-modified biochar obtained from the peanut shells. The adsorbent was modified with SDS of different concentrations. The obtained results showed that with the increasing surfactant concentration, the surface area accessible to adsorption increases. As a result, the Methylene Blue adsorbed amounts were considerably larger. The maximum adsorption capacity of the SDS-modified biochar as regards MB was 503 mg/g [74].

The SDBS and SDS anionic surfactants were applied for the magnetic biochars derived from the corncobs and furfural residue modification. The obtained adsorbents were used for norfloxacin (an antibiotic with bactericidal action) adsorption. It was proved that the surfactant modification increased the norfloxacin adsorbed amount. The SBDS with a small concentration showed a larger impact on antibiotic adsorption, whereas SDS with higher concentrations was more effective [41].

Magnetic biochars modified with the amphoteric surfactant-dodecyl dimethyl betaine (BS-12) were used for the phenanthrene adsorption. The adsorbed amount of phenanthrene BS-MC (a substance from the group of polycyclic aromatic hydrocarbons) decreased with the increasing BS-12 surface coating ratio. The change in the solution pH values caused no significant effects on the phenanthrene adsorption [75].

Triton X-100 (2-{4-(2,4,4-trimethylpentan-2-yl)phenoxy}ethanol) belongs to the group of non-ionic surfactants. It was used for the activated biochar derived from the horsetail herb modification. The obtained adsorbent was successfully applied for the poly(acrylic acid) polymer and toxic Pb(II) heavy metal adsorption from the aqueous solutions. It was shown that the PAA adsorbed amounts decrease on the surface of the modified biochar compared to the non-modified one, whereas the Pb(II) adsorption is more effective on the surface of the Triton X-100-modified adsorbent [76]. Poly(acrylic acid) was also adsorbed on the surface of the activated biochars obtained from the peanut shells and corncobs, modified with Triton X-100. The surfactant modification had a small impact on the PAA adsorbed amount. Moreover, the changes in the solution pH values (3, 6, 9) influenced the poly(acrylic acid) adsorbed amount more significantly compared with any adsorbent modifications with the surface active agent. The obtained maximum adsorbed amount of PAA on the Triton X-100-modified activated biochar was 55 mg/g [67].

The biochars obtained from the peanut shells used for the Bisphenol A removal were modified with the non-ionic surfactant Tween 20 (polyoxyethylene (20) sorbitan monolaurate). Its effect on Bisphenol A adsorbed amount was similar to that caused by the ionic surfactants (CTAB, SDBS). The adsorbed amount decreased by 10 times on the surface of the Tween 20-modified biochar in comparison to the non-modified one. The adsorption efficiency decreased with the increasing concentration of Tween 20 [68].

After the chemical activation, the biochars obtained from the eucalyptus sawdust were modified with three different non-ionic surfactants: PEG 2000 (polyethylene glycol), Pluronic P-123 (poly(ethylene glycol)-*block*-poly(propylene glycol)-*block*-poly(ethylene glycol)), and Pluronic F-127 (2-(2-(2-hydroxyethoxy)propoxy)ethanol)) and used for the adsorption of metronidazole (an antibiotic used to treat infections with anaerobic microorganisms and mixed flora with anaerobes). All of the examined surfactants (dissolved in ethanol) affected the solid porous structure. PEG 2000 and Pluronic P-123 increased the pore volume and its mean diameter, whereas Pluronic F-127 enhanced only the pore size. All the above surfactants had an impact on metronidazole adsorption. The antibiotic exhibited the greatest affinity for the surface of the adsorbent modified with PEG 2000 (removal 100%), whereas its adsorbed amount was the smallest on the surface of the Pluronic F-127-modified biochar (removal 80%) [77].

Table 3 summarizes the experimental conditions for the design and salient features of surfactant-modified biochar specimens, whereas Figure 10 presents the possible applications of surfactant-modified biochars.

### 3.5. Surface Arylation with Diazonium Salts

The chemistry of aryl diazonium salts dates back to the mid-1800s [78] and was at the origin of the industrial production of azo dyes [79]. It is also explored in numerous organic synthesis reactions [80]. Only since 1992 has it been applied worldwide to modify materials surfaces, particularly carbon allotropes [40,81]. This approach is alluring because of its commercially abundant comprising aromatic amines with various functional groups as diazonium precursors.

A general pathway for the modification of carbon materials is depicted in Figure 11. Mostly, the *ex situ* or *in situ* generated diazonium salt reacts in aqueous or organic solvents in order to provide radicals that attack the surface, or the diazonium forms a diazoether interfacial bond, followed by the release of dinitrogen and formation of C-O-C interface. An example is given for carbon surface-bearing surface functional groups.

Biochar is among these functionalized carbons and is thus prone to arylation with diazonium salts. The grafted aryl groups display scaffolds to link moieties through specific reactions as they possess suitable functional groups. They comprise amide coupling, coordination bonding, and click chemistry [55]. The surface-aryl bond is usually strong owing to its covalent nature, therefore ensuring remarkable mechanical properties of polymers reinforced with arylated fillers or strong adhesive bonding of polymers to arylated surfaces. One can also take advantage of the strong arylation of carbonaceous supports to anchor bimetallic nanocatalysts with excellent dispersion and narrow size distribution for nitrate electroreduction application [82].

**Table 3.** Summary of inorganic and organic compounds adsorption on the surfactant-modified biochar surface.

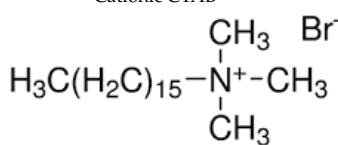
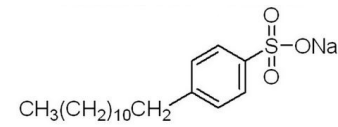
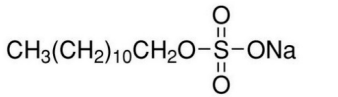
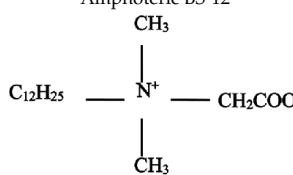
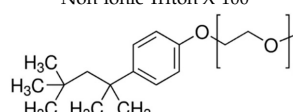
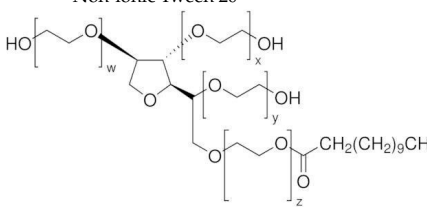
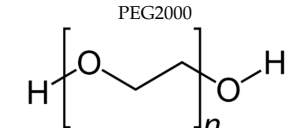
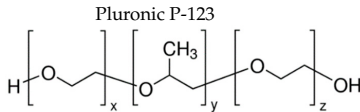
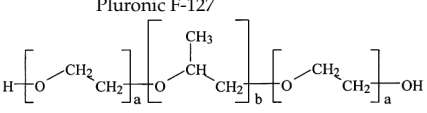
Surfactant	Biomass Used for Biochar Preparation	Surfactant Immobilization Conditions	Properties of Modified Biochar	Application	Reference
Cationic CTAB 	<i>Populus alba</i>	C <sub>0</sub> : 22 mg/L Dried at 105 °C	-	Cr(VI)	[65]
	Rice husk	C <sub>0</sub> : 1457 mg/L Dried at 60 °C	Surface charge change to positive	Inorganic nitrogen fertilizers removal	[66]
	Peanut shells Corncoobs	C <sub>0</sub> : 100 mg/L pH = 3, 6, 9	-	Poly(acrylic acid) adsorption	[67]
	Peanut shells	C <sub>0</sub> : 17–272 mg/L T: 25 °C pH: 6	-	Bisphenol A adsorption	[68]
	Coffee husk	C <sub>0</sub> : 2550 mg/L T: 30 °C Dried at 60 °C	Specific surface area decrease (from 750.1 to 557.4 m <sup>2</sup> /g) Pore volume decrease (from 0.3541 to 0.3192 cm <sup>3</sup> /g) Pore mean diameter increase (from 18.9 to 22.9 Å)	Reactive dyes removal	[69]
	Cornstalks	C <sub>0</sub> : 10 mg/L Dried at 60 °C Neutral pH	Surface charge change to positive	Orange II and methylene blue adsorption	[70]
	Anionic SDBS 	Rice husk	C <sub>0</sub> : 437.5 mg/L Dried at 60 °C	Surface charge change to negative	Inorganic nitrogen fertilizers removal
Peanut shells		C <sub>0</sub> : 24.5–392 mg/L T: 25 °C pH: 6	-	Bisphenol A adsorption	[68]
Cassava peels Corn cob Furfural residue		C <sub>0</sub> : 30–150 mg Dried at 110 °C C <sub>0</sub> : 61.25–3062.5 mg/L pH: 2–10	More numerous surface active sites availability	Methylene blue adsorption Norfloxacin adsorption	[72] [41]
Anionic SDS 		Peanut shells Corncoobs	C <sub>0</sub> : 100 mg/L pH: 3, 6, 9	-	Poly(acrylic acid) adsorption
	Peat	C <sub>0</sub> : 100 mg/L pH: 3, 4.5, 6, 9	-	Poly(acrylic acid) adsorption	[71]
	Cassava peels	C <sub>0</sub> : 30–150 mg/L Dried at 110 °C	-	Methylene blue adsorption	[73]
	Peanut shells	C <sub>0</sub> : 6–30 mg/L Dried at 65 °C	Specific surface area increase (from 51.37 to 85.62 m <sup>2</sup> /g) Pore volume increase (from 0.232 to 0.283 cm <sup>3</sup> /g) Pore mean diameter decrease (from 3.794 to 1.543 nm)	Methylene blue adsorption	[74]
	Corn cob Furfural residue	C <sub>0</sub> : 61.25–3062.5 mg/L pH: 2–10	-	Norfloxacin adsorption	[41]

Table 3. Cont.

Surfactant	Biomass Used for Biochar Preparation	Surfactant Immobilization Conditions	Properties of Modified Biochar	Application	Reference
Amphoteric BS-12 	-	Modification 25–200%	-	Phenanthrene adsorption	[75]
Non-ionic Triton X-100 	Horsetail herb  Peanut shells Corncobs	C <sub>0</sub> : 100 mg/L pH: 3  C <sub>0</sub> : 100 mg/L pH: 3, 6, 9	-	Poly(acrylic acid) and Pb(II) adsorption  Poly(acrylic acid) adsorption	[76]  [67]
Non-ionic Tween 20 	Peanut shells	C <sub>0</sub> : 3.5–56 mg/L T: 25 °C pH: 6	-	Bisphenol A adsorption	[68]
PEG2000 	Eucalyptus sawdust	Surfactant dissolved in ethanol T: 60 °C Neutral pH	Specific surface area decrease (from 462 to 448 m <sup>2</sup> /g) Pore volume increase (from 0.309 to 0.392 cm <sup>3</sup> /g) Pore mean diameter increase (from 2.679 to 3.497 nm)	Metronidazole adsorption	[77]
Pluronic P-123 	Eucalyptus sawdust	Surfactant dissolved in ethanol T: 60 °C Neutral pH	Specific surface area decrease (from 462 to 436 m <sup>2</sup> /g) Pore volume increase (from 0.309 to 0.3586 cm <sup>3</sup> /g) Pore mean diameter increase (from 2.679 to 3.289 nm)	Metronidazole adsorption	[77]
Pluronic F-127 	Eucalyptus sawdust	Surfactant dissolved in ethanol T: 60 °C Neutral pH	Specific surface area decrease (from 462 to 221 m <sup>2</sup> /g) Pore volume decrease (from 0.309 to 0.2465 cm <sup>3</sup> /g) Pore mean diameter increase (from 2.679 to 4.466 nm)	Metronidazole adsorption	[77]

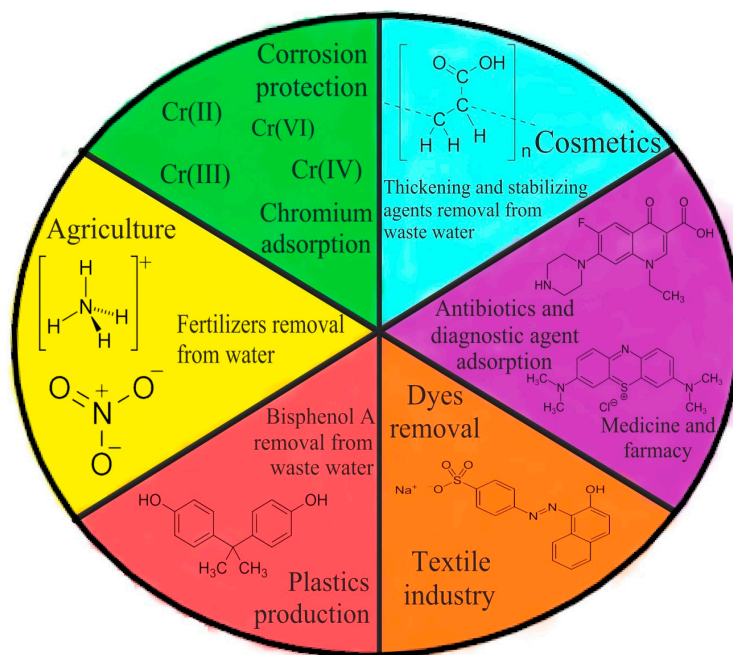


Figure 10. Applications of biochars modified by surfactants in various fields of human activity.

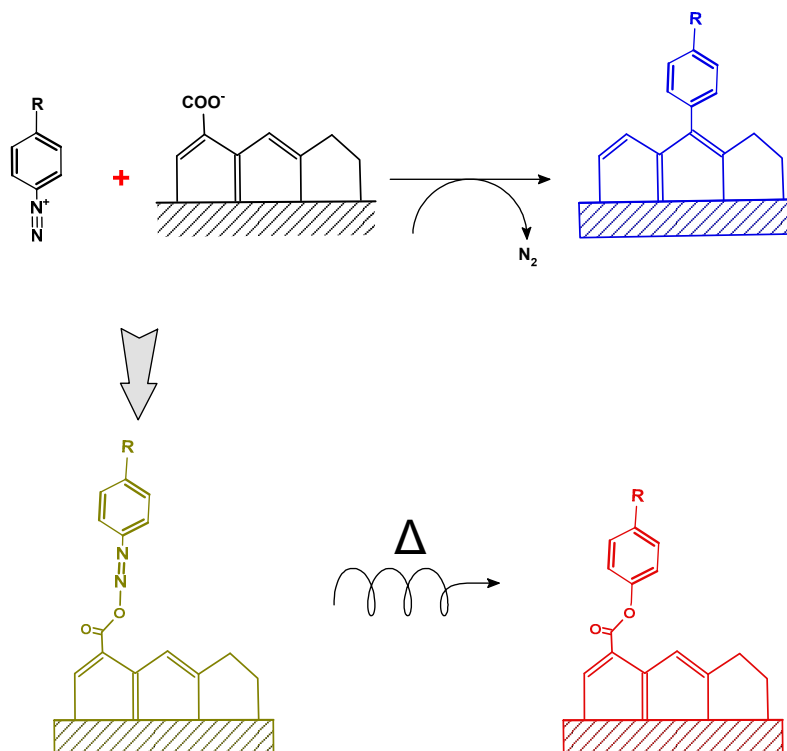
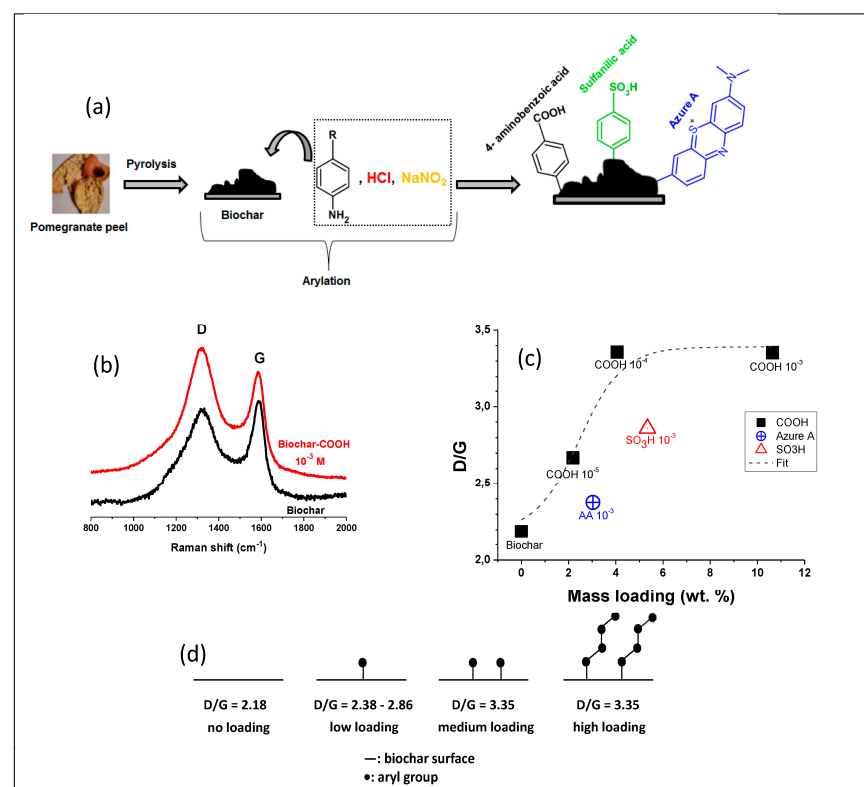


Figure 11. Schematic illustration of the modification of a graphitic surface with aryl diazonium salts.

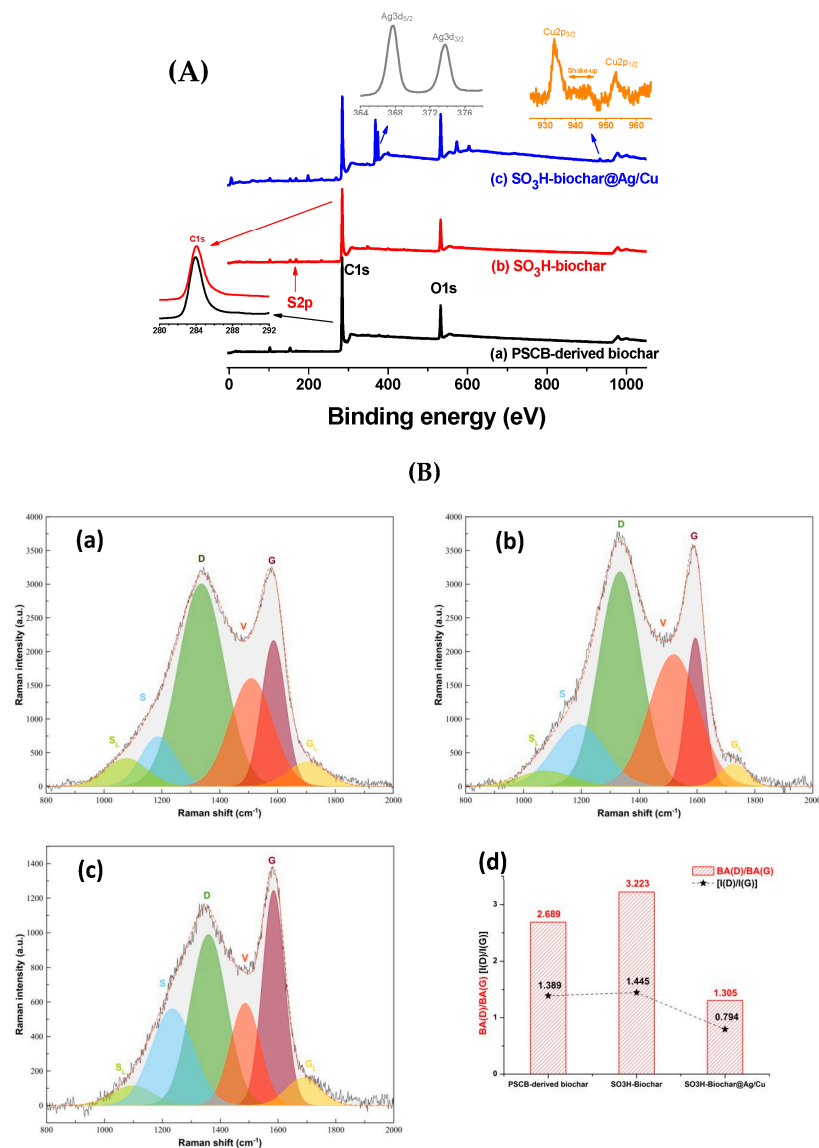
The arylation of carbon allotropes, including fullerene, graphene, and carbon nanotubes with diazonium salts, showed enhanced properties and performances in several domains such as electrocatalysis, sensing, and optics [55]. However, these precursors are expensive with limited large-scale applications. Alternatively, the obtained biochar from agrowaste pyrolysis can provide a highly porous matrix compared to the initial lignocellulosic materials [83]. Biochar can be treated with acids or alkalis to provide a higher surface area with an enhanced porous structure. Apple leave-derived char was activated through

various processes. This work study was concerned with investigating the impact of acid and thermal treatments on the physico-chemical properties of the resulting biochar. The latter was capable of abstracting the organic pollutants from water [84]. Several Raman spectra for carbonaceous matter seem to be complex. It may be referred to as the complicated structure they possess. The simplest spectrum is for graphite because of the uniformity of its formation showing planar and stratified laminates. Relative deformations may arise in this structure, expressing a weak D band with a directly proportional intensity to the extent of disorders in this structure. Khalil et al. [85] investigated fundamental variations in the D/G peak intensity ratio on going from the pristine biochar derived from pomegranate peels when compared to different arylated biochar samples, namely Biochar-COOH, biochar-SO<sub>3</sub>H, and biochar-Azure A. The results expressed that the D/G peak ratio grows with arylation without depending on the kind of diazonium compound. The intensity of Raman D/G peaks was correlated to the elementary concentration of the employed diazonium salts. Figure 12a depicts the general route for the arylation of pomegranate biochar with in situ generated three diazonium salts. Figure 12b compares the Raman bands of pristine and arylated biochar; the D/G intensity ratio increases upon treatment of diazonium salts, which is a sign of true covalent modification resulting from arylation. Figure 12c plots the D/G ratio as a function of the grafting extent determined by TGA. Interestingly, for similar high initial concentrations, Azure A induces marginal change in D/G intensity ratio due to steric hindrance. Figure 12d schematically illustrates the gradual change in the grafting density of aryl groups at the surface. High initial concentration is likely to result in oligomerization of the aryl groups [56,86], hence the tendency of the D/G intensity ratio to reach a plateau value. Indeed, chemical grafting reactions no longer affect the carbon allotrope support but the organic layer, previously attached [87].



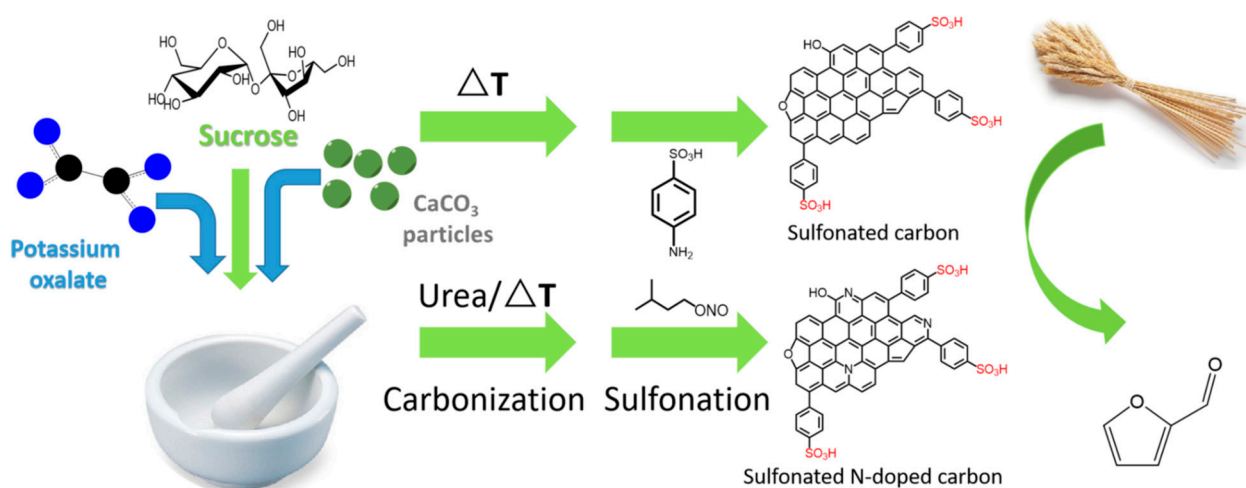
**Figure 12.** Arylation of pomegranate biochar: (a) modification with in situ generated diazonium salts, (b) Raman spectra of biochar and carboxyphenyl-modified biochar using a 10<sup>-3</sup> M aromatic amine solution, (c) plot of D/G vs. mass loading (wt.%) for different biochar samples, and (d) schematic illustration of stepwise growth of oligoaryl chains and their effect on D/G peak area ratio. Reprinted from [85] with permission of Springer Nature.

Snoussi et al. [88] prepared biochar from the pyrolysis of the pulp of sugarcane pulp bagasse (PSCB) at 500 °C and modified it with sulfanilic acid-based, in situ generated diazonium salts. AgCu bimetallic nanocatalyst was loaded by in situ reduction of the silver and copper nitrate-impregnated arylated biochar (SO<sub>3</sub>H-Biochar) using phytochemicals extracted from the biomass. Sulfonation and deposition of the bimetallic AgCu nanocatalysts were probed by XPS (Figure 13A). Raman spectra (Figure 13B) curve fitting permitted to determine D and G band area and height. This curve-fitting showed deformations in the carbon lattice resulting from the arylation process with some disorders when compared to the pristine biochar (Figure 13B(a,b)). A noticeable increase in biochar defects can be referred to the surface arylation (Figure 13B(b)), whereas a minor effect results in a slightly higher D/G band intensity ratio. However, upon metal deposition, a significant relative increase in the G band area or height and, thus, a decrease in the D/G band area or peak height intensity ratio suggested an increase in the graphitization, resulting in boosting the catalytic efficiency.



**Figure 13.** (A) XPS analysis of sugarcane bagasse biochar and related sulfonated biochar and biochar@Ag/Cu. (B) Curve fitting of Raman spectra of (a) sugarcane pulp bagasse (PSCB)-derived biochar, (b) SO<sub>3</sub>H-Biochar, (c) SO<sub>3</sub>H-Biochar@Ag/Cu, and (d) the evolution of BA(D)/BA (G) and I(D)/I(G) ratios based on the curve fitting calculations.

Arylation of the activated carbon with 4-sulfobenzene diazonium chloride was carried out for synthesizing 4-sulfophenyl activated carbon to act as an efficient catalyst. Changing the conditions of the reaction provided an arylated activated carbon with sulfanilic acid possessing numerous acid sites. The used catalyst was recovered easily upon utilizing it in esterification reactions of some fatty acids [89]. Bamboo-activated carbon was arylated by sulfanilic acid to produce heterogeneous catalysts. The prepared arylated catalysts showed high activity in esterifying oleic acid with alcohol. The microstructure shrinkage may lead to the deactivation of the heterogeneous acid catalyst. Meanwhile, the regenerated catalyst can be used, providing an efficiency of over 90% [90]. Sulfonated sucrose-based and N-doped activated carbon were prepared using N-source, pore-forming, and sulfonating agents to act as catalysts. They were then employed in producing furfural from wheat straw (Figure 14). One of these modified catalysts showed acceptable recyclability. The aromatic sulfanilic acid groups were successfully grafted onto the activated carbons via a simple sulfonation procedure [91].

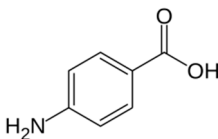
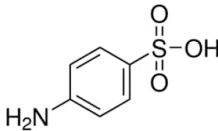
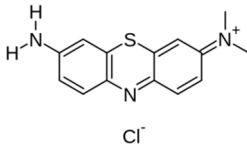


**Figure 14.** Schematic illustration of the preparation of sulfonated biochar as a catalyst of furfural production from wheat straw. Reproduced from [91] with permission of Elsevier.

In another study, sulfonated bio-carbon samples were prepared via partial carbonization of biomass-based substrates with sulfuric acid or diazonium salt. The performance of the catalysts relied upon the concentration of sulfonic acid groups [92]. Sulfonated carbon materials are covalently functionalized with sulfonic acid groups. They show promising efficiency and selectivity, surpassing traditional acid catalysts. The eminent performance of sulfonated carbonaceous substrates may be correlated to their distinctive topographical features, enhancing catalysis and selective adsorption [93]. Amino-arene-sulfonic acid was used to sulfonate biochar for producing a hydrophobic sulfonic acid functional biochar in a one-pot diazo-reduction process. The length of the arene chain and the grafting magnitude of arenesulfonic acid are substantial factors in monitoring the hydrophobicity of the functionalized biochar catalysts. The latter has a large surface area with an appropriate pore size distribution. This modified biochar supplies an active catalyst in many transformation reactions. These catalysts showed catalytic efficiencies in alkylating 2-methylfuran with cyclopentanone in biofuel production [94].

Table 4 gathers the salient features of some biochar samples arylated under diverse conditions and for various applications such as the catalyzed transformation of furfural or esterification reaction. Arylation is certainly of interest, but if it is conducted with a high initial diazonium concentration, it will lead to a sharp decrease in the specific surface area and the porous volume. Arylation with in situ generated diazonium salts requires a strong acidic medium, i.e., 25–37% HCl. This could favor the formation of a porous structure.

**Table 4.** Surface treatment of biochar with aryl diazonium salts.

Coupling Agent	Biomass	Surface Treatment Conditions	Properties of Engineered Biochar	Potential Application	References
	Pomegranate peel	Reaction with in situ generated diazonium salt, in 37% HCl, amine:NaNO <sub>2</sub> = 1:1; final diazonium concentration = 10 <sup>-5</sup> –10 <sup>-3</sup> M	Controlled arylation, mass loading = 2.2–10.6 wt/wt%, D/G = 2.7–3.4 (peak area ratio).	NA, potential heavy metal removal,	[85]
	Sugarcane bagasse	Reaction of 300 mg biochar with in situ generated diazonium salt, in 37% HCl, amine:NaNO <sub>2</sub> = 1:1 (6 mmol:6 mmol);	Arylation yields the grafting of 2 SO <sub>3</sub> per 100 biochar carbon atoms. D/G = 1.39 for biochar and 1.45 for biochar-SO <sub>3</sub> H. Arylation with in situ generated diazonium in concentrated HCl induces channel formation within the biochar.	In situ deposition of Ag(I) and Cu(II) ions, followed by reduction using sugarcane bagasse extract.	[88]
	Pomegranate peel	Reaction with in situ generated diazonium salt, in 37% HCl, amine:NaNO <sub>2</sub> = 1:1; final diazonium concentration = 10 <sup>-3</sup> M	Mass loading = 5.3%, D/G = 2.9 (peak area ratio)	NA, potential heavy metal removal	[85]
	Bamboo  Sucrose-K <sub>2</sub> C <sub>2</sub> O <sub>4</sub> •H <sub>2</sub> O-CaCO <sub>3</sub> -Urea (1-1-1-0 or 1-1-1-0.5 wt.fractions)	Sulfanilic acid/Biochar molar ratio = 0.1–1.5, in 25% HCl, at 30–80 °C, for 2–60 min. Biochar prepared at 600–800 °C without urea, and at 750 °C in the presence of urea. 1 g biochar mixed with 4 g sulfanilic acid and 2 g isoamyl nitrite, in 150 mL DIW. Arylation at 80 °C overnight.	Total acid density = 1.69 mmol/g. SSA decreased from 919 to 225 m <sup>2</sup> /g upon arylation. Drastic reduction of SSA from 1422 to 190 m <sup>2</sup> /g for biochar prepared at 800 °C, and from 1658 to 30 m <sup>2</sup> for biochar-urea and sulfonated biochar-urea. Sulfur content: 0.08 to 2.29 mmol/g. With urea, very high arylation D/G increased with arylation.	Acid catalyst. Up to 96% catalyzed esterification of oleic acid with ethanol.  Catalytic furfural production from wheat straw.	[90]  [91]
	Pomegranate peel	Reaction with in situ generated diazonium salt, in 37% HCl, amine:NaNO <sub>2</sub> = 1:1; final diazonium concentration = 10 <sup>-3</sup> M	Mass loading = 5.3%, D/G = 2.9 (peak area ratio)	NA, potential radical polymerization photoinitiation	[85]

APTES: aminopropyl triethoxysilane; DIW: de-ionized water; SSA: specific surface area.

### 3.6. Surface-Modified Biochar with Nitrogen-Based Compounds

Owing to the versatility of  $sp^2$  carbon surface and the availability of highly interacting functional groups, biochar is prone to molecular and macromolecular post-functionalization with aminated compounds. Doping biochar with nitrogen-containing compounds during pyrolysis or hydrothermal treatment of the biomass is out of the scope of this review, and the reader is referred to selected articles on the topic [95–97]. Similarly, strong activation with nitric acid to provide surface amino groups is covered but not with a dedicated section; for example, see the work of Bamdad et al. [98].

Modification can proceed with a molecular coupling agent or with the adsorption of a monomer that is subjected to polymerization.

Two major nitrogen-containing compounds have been employed to modify the surface of biochar: aniline and 2-aminothiophenol-related compounds and polyethyleneimine (PEI). The aniline derivatives are usually subjected to in situ oxidative polymerization in the presence of biochar. Surface-confined polymerization proceeds with the adsorption of the aniline derivative, most probably driven by biochar-COOH ...  $H_2N-C_6H_4-R$  hydrogen bonding. For example, 2-aminothiophenol can be adsorbed on the surface of biochar and subjected to oxidative polymerization using ammonium persulfate to yield poly(2-aminothiophenol)-coated biochar particles (Figure 15) [99]. Note that, in Figure 15, hydrogen bonds are shown for N ... N interactions; in our fair opinion, hydrogen bonds occur between  $NH_2$  from the monomer and the COOH and/or OH from the biochar surface. Indeed, Lewis acid–base interactions, or more particularly, hydrogen bonds, are maximized for COOH- $NH_2$  rather than  $NH_2-NH_2$  interactions [100]. The biochar composite was tested for the uptake of Hg and As from wastewater and was found to remove over twice as many contaminants, at pH 9, compared to the untreated biochar. Adsorption leveled off at ~32 and 119 mg/g As(III) and Pb(II), respectively. These values are much higher than those recorded with unmodified biochar (14 and 47 mg/g for AS(III) and Pb(II), respectively). At this stage, it is essential to note that despite a drastic two-fold decrease in the specific surface area of the engineered biochar owing to the polymer coating (118 and  $59\text{ m}^2/\text{g}$  for engineered and pristine biochar, respectively), the removal of As(III) and Pb(II) remained high.

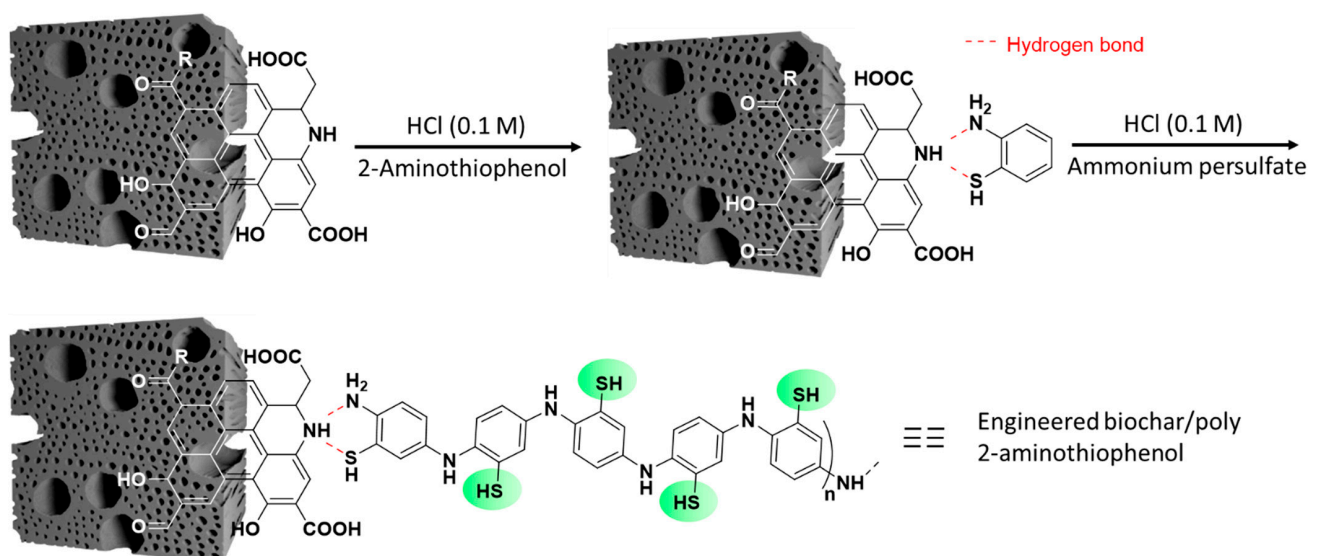


**Figure 15.** Schematic illustration of the route to engineered biochar/poly(2-aminothiophenol) adsorbent via in situ oxidative polymerization of 2-aminothiophenol. Reproduced from [99] with permission of Elsevier.

Aniline is a much more investigated monomer to provide composites of biochar and polyaniline (PANI). It can be synthesized in the presence of biochar and remains glued to the latter via hydrogen bonds (Figure 16).

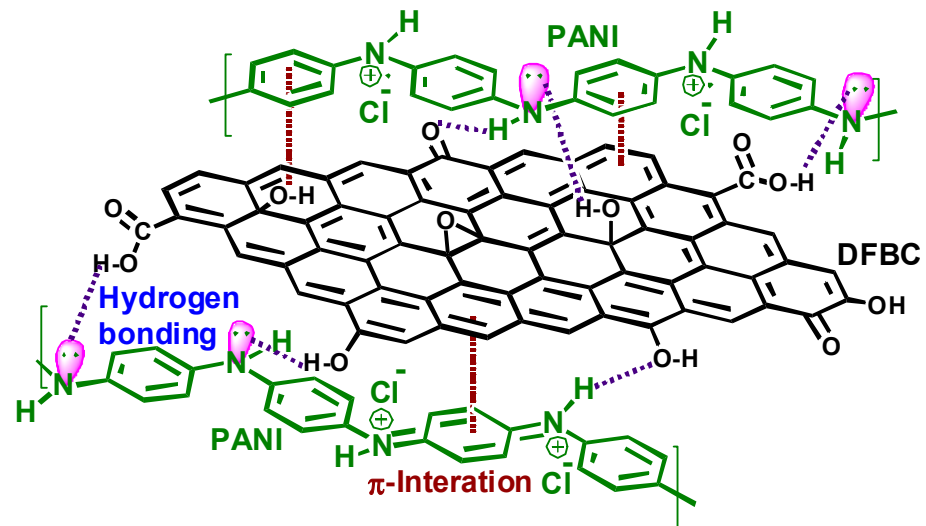


**Figure 16.** Biochar-PANI composite chemical structure. Dotted lines indicate hydrogen and p-p bonds between biochar and the PANI deposit. Reproduced from [101] with permission of Elsevier.

Douglas fir biochar was prepared by fast pyrolysis at 900–1000 °C and served for the in situ deposition of PANI by oxidative polymerization [101]. 1 g biochar-PANI composite removed 150 mg Cr(VI) and 72 mg nitrates, at pH 2 and 6, respectively, much more than the pristine biochar. PANI provides nitrogen-based anchoring sites for Cr(VI) and hydrogen bonding acceptors from biochar OH and COOH groups.

Magnetic biochar-PANI composites were prepared by wet impregnation of durian rind powder with three iron precursors, followed by pyrolysis at 800 °C. The resulting magnetic biochars were further coated with PANI via in situ oxidative polymerization of aniline using ammonium persulfate, in an acidic medium (1 M HCl), at 0–5 °C. The highest specific surface was 855 m<sup>2</sup>/g. The magnetic biochar prepared using FeCl<sub>3</sub>·6H<sub>2</sub>O precursor and topped with PANI was used as a supercapacitor; it exhibited a specific capacitance of 615 F/g at 10 mV/s and an energy density of 76.9 Wh/kg [102].

Magnetic banana stem biochar was prepared in situ deposition of magnetite after the carbonization process of the biomass at 500 °C. PANI was prepared by in situ polymerization to yield a supercapacitor composite material that has a specific capacitance  $C_s = 315.7 \text{ Fg}^{-1}$ , higher than that of the magnetic biochar without any PANI ( $C_s = 234.8 \text{ Fg}^{-1}$ ) [103].

Tobacco biochar was fabricated, treated with phosphoric acid, and mixed with PANI, then Ag<sub>3</sub>PO<sub>4</sub> was synthesized in situ. The final Biochar/PANI/Ag<sub>3</sub>PO<sub>4</sub> was employed as a photocatalyst to degrade triclosan [104]. The rationale for making this ternary composite lies in the synergy between (i) the excellent photocatalytic properties of Ag<sub>3</sub>PO<sub>4</sub>, (ii) the electronic conductivity of biochar that favors the rapid transfer of photogenerated electron (e<sup>-</sup>) of Ag<sub>3</sub>PO<sub>4</sub>, and (iii) PANI, a promoter of the transfer and separation of photogenerated hole-electron pairs (h<sup>+</sup>-e<sup>-</sup>), as well as an inhibitor of the photo-corrosion and oxidation of Ag<sub>3</sub>PO<sub>4</sub>. The composite catalyzed the degradation of triclosan at a rate of 85% within 10 min.

Another type of biochar/polymer composites can be prepared by mixing biochar with PEI, using methanol or ethanol [105–109]. Electrostatic interaction between the protonated amino groups from the biochar and the carboxylate groups from biochar can take place. Further, strong hydrogen bonds are expected. Covalent grafting of PEI could be achieved using glutaraldehyde [43,110] or EDTA dianhydride [106]. For example, the frequently em-

employed glutaraldehyde is a good coupling agent as it reacts with OH functional groups [111] from biochar surface and the NH/NH<sub>2</sub> groups from PEI. An example of a composite is illustrated in Figure 17, showing the fabrication of magnetic biochar-PEI nanocomposite employed for the removal of Cr(VI).

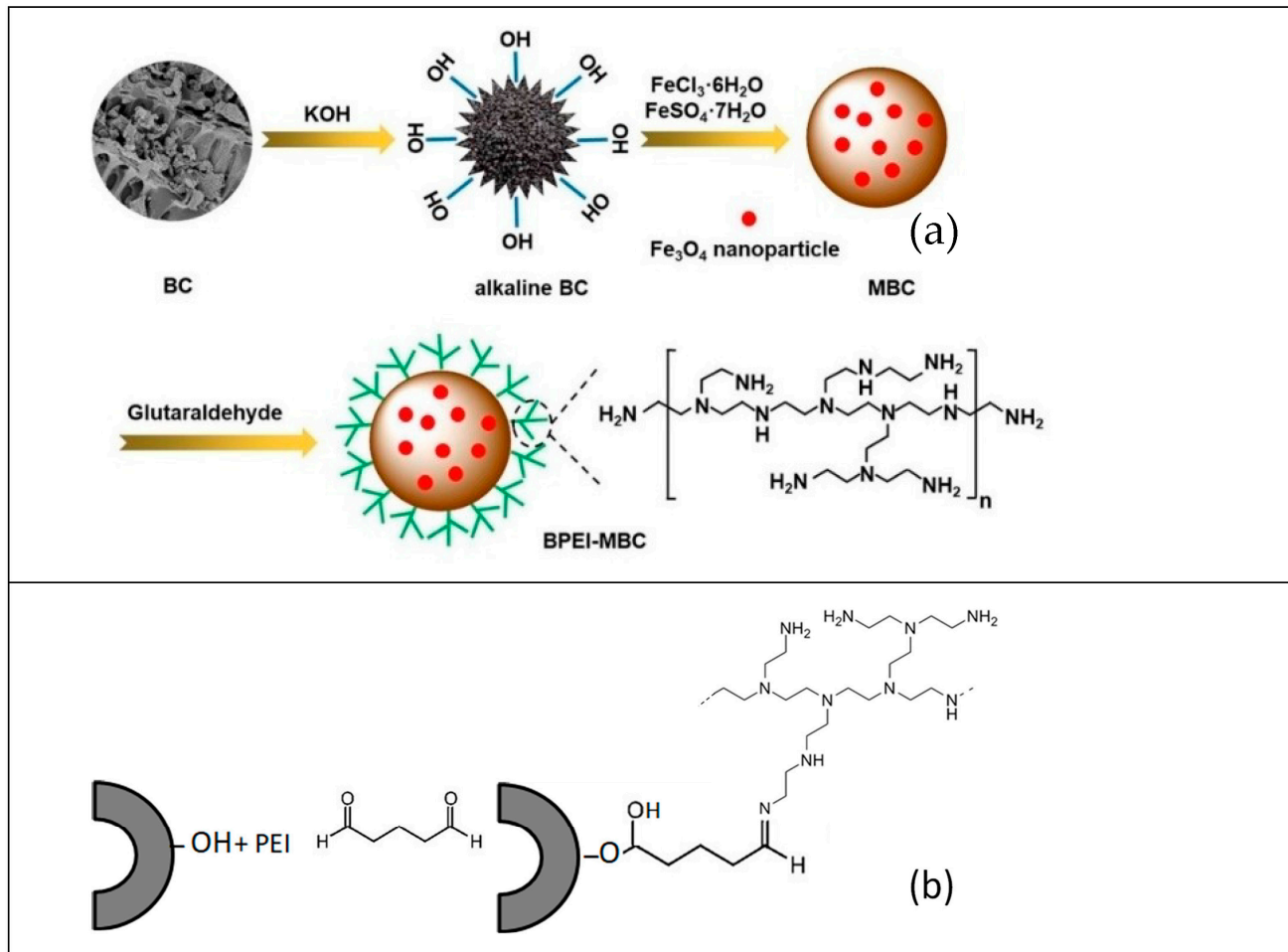


**Figure 17.** Schematic illustration of the fabrication of magnetic coconut shell biochar and its graft modification with PEI (a). Use of glutaraldehyde for coupling PEI to the underlying biochar (b). Figure 17a reproduced from with permission of Wiley & Sons.

As a few examples of the performance of PEI-modified biochar materials, PEI-modified pine needles biochar enabled the ability to adsorb 294 mg/g Congo Red, almost 10-fold the adsorption capacity of the pristine biochar (30.8 mg/g) [112].

PEI-modified biochar was employed for the detoxification of Cr(VI); it was found to remove 435.7 mg per g of biochar, nearly 20 times higher than 23.1 mg/g for pristine biochar [105].

Table 5 reports experimental conditions, properties, and applications of shortlisted biochars modified with nitrogen-containing molecules and macromolecules.

**Table 5.** Surface treatment of biochar with nitrogen-based compounds.

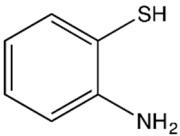
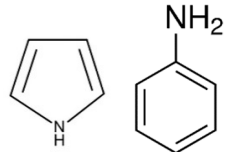
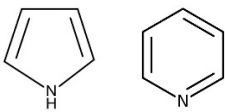
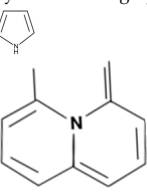
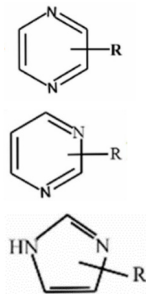
Coupling Agent	Biomass	Surface Treatment Conditions	Properties of Engineered Biochar	Potential Application	References
poly 2-aminothiophenol 	Date leaves	Reaction of 1000 mg date leaves biochar within 2-aminothiophenol (0.5 mL), in 0.1 M HCl, 20 mL of a solution (0.1%) of ammonium persulfate.	SSA 59.02 m <sup>2</sup> /g, Average pore diameter 20.16 nm	Removal of arsenic and mercury ions from wastewater	[99]
pyrrole/aniline 	Forestry waste	Co-polymerization of polypyrrole/polyaniline on ferrate-modified biochar. pyrrole/aniline (Volume ratios = 0:1 (0, 1 mL) – 1:0 (1, 0 mL) and 1 g CTAB were added into the above solution with HCl of 1 mol/L.	SSA 56.97 m <sup>2</sup> /g Pore-size distributions 17.98 nm	Adsorption of hexavalent chromium in water	[113]
pyrrolic- and pyridine-like N 	Birch tree	Birch trees/H <sub>3</sub> PO <sub>4</sub> (50 wt.%)/melamine weight ratio of 1:4:3 at 800 °C, for 1 h.	SSA dominated by mesopores (86.4%), nitrogen functional groups with 5.4% of N in its structure D/G = 2.0.	Adsorption of acid red 18 dye.	[114]
pyrrolic N and graphitize N 	Pomelo peel	Reaction with one-pot pyrolysis, Pomelo peel powder, NaHCO <sub>3</sub> and melamine at a mass ratio of 1:3:4, 600–900 °C	Specific surface area 738 m <sup>2</sup> /g, nitrogen content 13.54 at%. D/G = 0.96	Removal of sulfamethoxazole	[115]
	Rice husk	Rice husk: urea mass ratio = 1:3, sonicated for 1 h, pyrolyzed at 800 °C	N-atom content = 8.11%, D/G = 1.095. Nitrogen doping decreased the number of defects in the biochar.	Catalytic degradation of dimethomorph	[116]
	Pistachio shells	10 g of pistachio shell as the carbon source, 2 g of melamine as the nitrogen source, and 5 g of NaHCO <sub>3</sub> /K <sub>2</sub> CO <sub>3</sub> as the activator.	SSA increased by about 1000 m <sup>2</sup> g <sup>-1</sup> after N-doping, the surface N content increased by more than 3%, and hydrophilicity and polarity declined.	Selective adsorption of toluene under humid conditions	[117]

Table 5. Cont.

Coupling Agent	Biomass	Surface Treatment Conditions	Properties of Engineered Biochar	Potential Application	References
the formation of abundant N-containing functionalities in the form of C-N, C=N and N-H in C-N polymer structures.	Melon seed shell	Melon seed shell/melamine Weight ratio = 1:1, in solvent (water and CH <sub>3</sub> CH <sub>2</sub> OH with a mass ratio of 1:1), Dried and pyrolyzed at 400 °C.	D/G = 0.71 (peak area ratio), formation of mesopores structure, average pore size of 12.6 nm, melamine or its derivatives reacted with the C=O functionality on the biochar, forming the C-N, C=N, and N-H bond on the biochar. Biochar became hydrophilic after introducing nitrogen species	Photocatalytic production of hydrogen	[118]
C-N, amino groups	Camellia oleifera shells	Pretreating biomass with (NH <sub>4</sub> ) <sub>2</sub> S <sub>2</sub> O <sub>8</sub> 50 g of the Camellia oleifera shells powder was added to 100 mL of ammonium persulfate (1 mol L <sup>-1</sup> ) until dry, and then placed into a N <sub>2</sub> atmosphere for pyrolysis at 700 °C.	SSA increased from 134.9 m <sup>2</sup> g <sup>-1</sup> to 739.9 m <sup>2</sup> g <sup>-1</sup> , and the pore volume also increased from 0.301 cm <sup>3</sup> g <sup>-1</sup> to 0.588 cm <sup>3</sup> g <sup>-1</sup> after introduce N-containing groups, pretreatment with (NH <sub>4</sub> ) <sub>2</sub> S <sub>2</sub> O <sub>8</sub> introduces various polar nitrogen-containing and sulfur-containing functional groups into biochar.	The adsorption capacity for Cu(II) and tetracycline.	[119]
pyridinic-N (N-6), pyrrole/pyridine-N (N-5), and quaternary-N (N-Q)	coconut shell	Coconut shell/urea (Mass ratio of 1:1) by the thermal activation at 873 K for 2 h, and the medium temperature ionic liquid of molten alkali KOH (85% purity, the mass ratio to the intermediate material was 1.5:1)	SSA increased from 594.8 to 1711.4 m <sup>2</sup> g <sup>-1</sup> , total pore volume increased from 0.31 to 0.80 cm <sup>3</sup> /g, mean pore size after nitrogen doping	The capacity of CO <sub>2</sub> adsorption can be up to 7.6 mol/kg at 273 K and 100 kPa.	[120]
pyridinic-N (N-6), pyrrole/pyridine-N (N-5), and quaternary-N (N-Q)	coconut shell	carbonization of coconut shell followed by urea modification and K <sub>2</sub> CO <sub>3</sub> activation at 600 °C (K <sub>2</sub> CO <sub>3</sub> /precursor ratio of 3)	SSA 1082 m <sup>2</sup> g <sup>-1</sup> , nitrogen content (wt%) 2.74	CO <sub>2</sub> capture capacity of 3.71 mmol/g at 25 °C	[121]
	Cellulose	Reaction with co-pyrolysis experiments of cellulose and nitrogen carriers (urea and chitosan), nitrogen carrier/(cellulose + nitrogen carrier) = 40–60%, at 350–750 °C.	The N groups on nitrogen-containing biochar were mainly Pyridine nitrogen and pyrrole nitrogen groups, the N atom was fixed in the carbon lattice.	Donor performance and conductivity of carbon materials.	[122]

SSA: specific surface area.

### 3.7. Modification of Biochar with Catalyst Nanoparticles

Biochar is a very versatile platform for nanocatalyst immobilization. This is a hot topic of interest for environmental and other applications such as organic synthesis. Our primary goal was to focus on biochar with molecular and macromolecular compounds. However, as most of the nanocatalysts immobilized on biochar were obtained from metal ion compounds, this section closes the review with a logical sequence when one considers the size: molecules, macromolecules, and nano- or macroparticles. Figure 18 summarizes the main methods of preparation of biochar loaded with catalytic particles:

- Method (i) consists in impregnating the initial biomass with catalyst precursor prior to pyrolysis. This process yields biochar powder impregnated with nanoparticles [37,123–125].
- Method (ii) concerns the deposition of catalyst precursor onto prefabricated biochar, followed by in situ reductive process to obtain biochar-immobilized nanocatalysts [8,88,126].
- Method (iii) is based on a simple mixture of prefabricated biochar and catalysts [7,127].

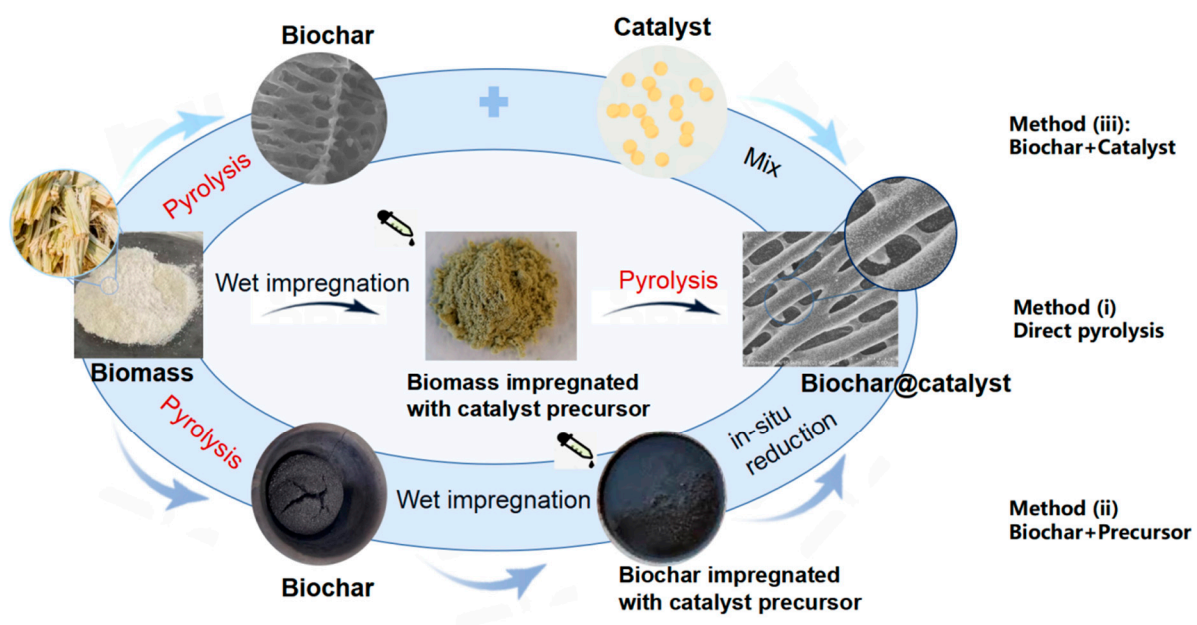


**Figure 18.** Main methods of surface modification of biochar with immobilized nanocatalysts.

From the own experience of the authors, Method (i) yields no loss and evenly dispersed nanoparticles in the nanoscale regime. It requires simple wet impregnation prior to pyrolysis. Method (ii) usually combines two processes: pyrolysis in dry conditions, followed by adsorption of metal ions and their in situ reduction by “beaker chemistry”. Method (iii) is perhaps the one that is amenable to pilot or higher scale process as it requires mixing two preformed components of the final composites. However, agglomerated catalyst nanoparticles might be difficult to disperse, with small size, over the biochar surface. Table 6 provides the summarized experimental work for the preparation of catalyst-modified biochar and potential applications of the shortlisted systems.

**Table 6.** Shortlisted biochar@catalyst composites prepared by three main routes, their properties, and applications.

Preparation Method	Biomass	Biochar@Catalyst (Size of Catalyst)	Synthesis Procedure	Pollutant Removal Efficiency	Refs.
Method (i) Pyrolysis of catalyst precursor-impregnated biomass	Olive pit powder (OP)	Biochar@CuNi (10–20 nm agglomerated into raspberry-shaped particles of CuNi)	Pyrolysis of OP pre-modified with citric acid, then impregnated with copper and nickel Ni nitrates before pyrolysis at 400 °C (1h/N <sub>2</sub> ).	Methyl Orange (MO) dye reduction using NaBH <sub>4</sub> . R <sub>eff</sub> = 75% within 90 min.	[128]
	Maize straw (MS)	Biochar@Cu(0) (Cu(0) nanoparticle size: NA)	1g MS was modified with 2.5 mmol CuCl <sub>2</sub> ·2H <sub>2</sub> O prior to pyrolysis at 700 °C (under N <sub>2</sub> . Pyrolysis duration: NA)	Enrofloxacin mineralization using 2 mmol/L PMS. Complete removal: 30 min for 10 mg/L of ENR at pH 3, using 0.3 g/L catalyst.	[125]
	Brewer spent grain (BSG)	Biochar@Ag-Cu (Ag-Cu nanoparticle size ≤ 80 nm)	1g of BSG powder was impregnated with 169.8 mg silver nitrate and 241.6 mg copper (II) nitrate trihydrate in 10 mL aqueous solution. The impregnated BSG powder was dried at 60 °C overnight and pyrolyzed at 500 °C (1h/N <sub>2</sub> ).	Study of the dual mineralization of MO and Methylene Blue (MB) dye mixture via advanced oxidation process. Total mineralization was observed for MO in less than 6 h.	[124]
Method (ii) In situ synthesis of nanocatalyst in the presence of Biochar	Sugarcane bagasse (SCB)	Biochar-SO <sub>3</sub> @AgCu (AgCu < 100 nm)	Pyrolysis of macerated SCB at 500 °C (1h/H <sub>2</sub> 5%/N <sub>2</sub> 95%), followed by arylation with diazonium salt in acidic medium. Biogenic AgCu nanocatalyst was prepared in the presence of the arylated biochar.	Mineralization of Malachite Green (MG) in the presence of H <sub>2</sub> O <sub>2</sub> . R <sub>eff</sub> = 80% within 50 min.	[88]
	<i>Camellia oleifera</i> shell powder	Biochar@Ce-Ag	CSP mixed with KOH and then pyrolyzed at 837 °C. 1g biochar was stirred with 0.458 g AgNO <sub>3</sub> , and 0.375 g Ce(NO <sub>3</sub> ) <sub>3</sub> ·6H <sub>2</sub> O for 1h, dried and pyrolyzed at 600 °C.	Sulfathiazole adsorption at 25 °C = 262 mg/g Biochar@Ce-Ag. Adsorption on pure CSP biochar = 42.4 mg/g.	[126]
Method (iii): Preparation of Biochar@Catalyst by mixing Biochar and catalyst	Pomegranate shell	Biochar@CuNi	Biochar was prepared in two steps: hydrothermal treatment at 180 °C/24 h followed by pyrolysis of the resulting hydrochar at 500 °C (1 h). CuNi bimetallic catalyst was prepared from equimolar mixture of copper and nickel chlorides. 0.5 g CuNi and 1 g biochar were mixed in 30 mL water under sonication for 30 min. The mixture was treated in autoclave at 140 °C for 12 h. The biochar@CuNi was dried at 80 °C for 4 h.	Application to the catalysis of A3 coupling reaction (A3: coupling reaction of an aldehyde, an amine, and a terminal alkyne). Optimal conditions were found in toluene, at 80 °C at reflux, for 8 h. Benzaldehyde (1.0 mmol), Mopholine (1.2 mmol) and Phenylacetylene (1.5 mmol) were reacted in the presence of 20 mg Biochar@CuNi. Highest yield = 88%.	[7]
	Bamboo	ZnO/Biochar	15 g bamboo was pyrolyzed, 600 °C, 2 h, N <sub>2</sub> . Biochar and ZnO particles were ball milled.	Photocatalytic degradation of MB (160 mg/g). Removal efficiency = 95.19%	[127]

#### 4. Conclusions

In this review, we have summarized the essential findings on the (macro)molecular and nanoparticulate levels of biochar surface treatment. We have covered the modifications of numerous biochar types with silane and titanate coupling agents, aryl diazonium salts, ionic and non-ionic surfactants, nitrogen-containing compounds, and nanocatalysts. Nitrogen species could be a polymerizable monomer (aniline derivatives) or a preformed polymer such as polyethyleneimine (PEI) adsorbed from an alcoholic solution.

One could draw numerous conclusions:

- In general, surface modification reduces the specific surface area and porous volume, but it is worth it because it imparts functionalities that unmodified biochar samples do not possess.
- Silanization requires rich oxygen functionalities at the surface, which could be obtained at moderate pyrolysis temperature or after oxidization of the biochar.
- Titanate could be envisaged to create new biochar-polymer composites if the primary intention is not to design biochar-titania photocatalysts.
- Aryl diazonium salts could be regarded as new coupling agents in materials surface chemistry as witnessed over the last three decades; their use to modify biochar particles is recent and very encouraging. Some of us have demonstrated that surface modification is limited by steric hindrance effects of the aryl group, and change in the carbon structure of the biochar is significant at low initial diazonium concentration.
- Modification with non-ionic and ionic surfactant adsorbed layers influences the textural characteristics of biochar, as well as acid–basic and hydrophilic–hydrophobic properties of its surface, changing the affinity for other substances present in the aqueous phase. The electrostatic, hydrogen bonds,  $\pi$ - $\pi$  electrons, and hydrophobic interactions are responsible for the surfactant molecules binding and can result in the formation of more complex surface structures, such as surfactant-adsorbate multilayers and micelles.
- The preparation of biochar-polyaniline composites is investigated by several researchers, particularly for the fabrication of supercapacitors, whereas poly(2-aminothiophenol) could be a remarkable alternative to provide surface-immobilized NH and SH groups able to chelate metal ions for environmental remediation issues.
- Polyethyleneimine is a nitrogen-rich polymer and could be coated on biochar particles by adsorption from methanol or ethanol solution. Tight, covalent immobilization and crosslinking require using organic coupling agents such as glutaraldehyde.
- Other attractive nitrogen-modification of biochar rest on the doping with ammonium persulfate or urea prior to pyrolysis, with a result of enhancing pyridinic, pyrrolic, and graphitic nitrogen in the biochar structure.
- Finally, there are numerous routes for catalytic nanoparticle modification of biochar groups in three major methods. They provide surface-immobilized nanoparticles, but pyrolysis of catalyst precursor-impregnated biomass seems to provide narrow-size distribution nanoparticles that are immobilized both at the surface and into the large pores of the biochar.
- These are the most investigated surface modifiers, but others are worth deeper insight, e.g., mercaptoethanol [129] and vitamin B6 [130]. Nevertheless, all in one, there is much to anticipate from a surface chemical modification of biochar in the coming years. Surface modification imparts remarkable new functionalities such as pollutant adsorption, immobilization of catalysts, and improved energy storage properties, to name but a few.

Concerning bulk, surface, and textural properties, we witnessed recurrent utilization of XPS, Raman and FTIR, XRD, nitrogen adsorption (for BET and porous volume), and TGA. Other techniques are also applied in the case of specific applications such as energy storage, namely DC voltage–current measurements and cyclic voltammetry. Ironically, we have noted that the biochar topic tackles the valorization of wastes with zero value but

requires a high number of analytical techniques, which is excessively costly for academic laboratories.

From the above, the conversion of agro- and other organic wastes into biochar is a very hot topic, with over 5500 publications per year. This will continue to grow in this era of economic crisis, on the one hand, and address some of the 17 sustainable development goals, on the other hand. We thus expect even more publications on the topic and the valorization of numerous other wastes. There are already, and there will be new regional niches from north to south to valorize biomasses such as Douglas fir, [101] brewer spent grain [124], sugarcane bagasse [88], olive [128,131] and date [132] stones, durian [102], etc. However, more rationality is needed to select which agrowaste is worth the thermochemical transformation into biochar by determining the initial cellulose-hemicellulose-lignin composition as their thermochemical transformation yields biochars with completely different properties and thus different potential applications, for example, as electrode materials [13]. Pyrolysis is interesting and offers advantages, but for other applications, hydrochars could be a solution because the treatment is faster, and the process might provide extraction of phytochemicals useful for reductive reaction processes [15] and also carbon dots [133]. Recently, microwave heating has emerged as an alternative for the fabrication of carbonaceous chars, with low energy cost of preparation, and remarkable properties [132]. Yet, when it comes to surface modification, this review has indicated numerous opportunities, but also challenges to overcome, such as the balance between surface chemistry and textural properties in order to achieve the desired end properties and performances.

**Author Contributions:** Conceptualization (A.M.K., M.W. and M.M.C.); Methodology (M.M.C. and M.W.); Validation (all authors); Writing—Original Draft (A.M.K., M.W. and M.M.C.); Writing—Review and Editing (all authors); Resources (M.M.C., A.M.K. and M.W.); Supervision (M.M.C.); Funding Acquisition (A.M.K., M.T., M.M.C., A.K.B. and Y.S.). All authors have read and agreed to the published version of the manuscript.

**Funding:** A.M.K. and M.M.C. would like to thank the French Government for funding AMK's contribution through a fellowship granted by the French Embassy in Egypt (Institut Francais d'Egypte). We thank the China Scholarship Council for the provision of Ph.D. scholarship to Mengqi Tang (No 202008310221). AKB thanks WBI for the provision of a grant, "Bourse Wallonie-Bruxelles International Excellence World (N° imputation-101386, and Article Budgetaire-33.01.00.07)".

**Institutional Review Board Statement:** Not applicable.

**Informed Consent Statement:** Not applicable.

**Data Availability Statement:** Not applicable.

**Conflicts of Interest:** The authors declare no conflict of interest.

## References

1. Adhikari, S.; Timms, W.; Mahmud, M.A.P. Optimising water holding capacity and hydrophobicity of biochar for soil amendment—A review. *Sci. Total Environ.* **2022**, *851*, 158043. [CrossRef]
2. Wijitkosum, S. Biochar derived from agricultural wastes and wood residues for sustainable agricultural and environmental applications. *Int. Soil Water Conserv. Res.* **2022**, *10*, 335–341. [CrossRef]
3. Harussani, M.; Sapuan, S. Development of Kenaf Biochar in Engineering and Agricultural Applications. *Chem. Afr.* **2021**, *5*, 1–17. [CrossRef]
4. Liu, H.; Liu, Y.; Li, X.; Zheng, X.; Feng, X.; Yu, A. Adsorption and Fenton-like Degradation of Ciprofloxacin Using Corncob Biochar-Based Magnetic Iron–Copper Bimetallic Nanomaterial in Aqueous Solutions. *Nanomaterials* **2022**, *12*, 579. [CrossRef]
5. Mukherjee, A.; Goswami, N.; Dhak, D. Photocatalytic Remediation of Industrial Dye Waste Streams Using Biochar and Metal-Biochar Hybrids: A Critical Review. *Chem. Afr.* **2022**, *6*, 609–628. [CrossRef]
6. Rodríguez Molina, H.; Santos Muñoz, J.L.; Domínguez Leal, M.I.; Reina, T.R.; Ivanova, S.; Centeno Gallego, M.Á.; Odriozola, J.A. Carbon Supported Gold Nanoparticles for the Catalytic Reduction of 4-Nitrophenol. *Front. Chem.* **2019**, *7*, 548. [CrossRef] [PubMed]
7. Zarei, M.; Saidi, K.; Sheibani, H. Preparation and investigation of catalytic activities of Cu-Ni nanoparticles supported on the biochar derived from pomegranate shells in the A3-coupling reactions. *Biomass Convers. Biorefin.* **2022**, 1–13. [CrossRef]

8. Santos, J.L.; Sanz-Moral, L.M.; Aho, A.; Ivanova, S.; Murzin, D.Y.; Centeno, M.A. Structure effect of modified biochar in Ru/C catalysts for sugar mixture hydrogenation. *Biomass Bioenergy* **2022**, *163*, 106504. [[CrossRef](#)]
9. Bartoli, M.; Arrigo, R.; Malucelli, G.; Tagliaferro, A.; Duraccio, D. Recent advances in biochar polymer composites. *Polymers* **2022**, *14*, 2506. [[CrossRef](#)]
10. Bélanger, N.; Prasher, S.; Dumont, M.-J. Tailoring biochar production for use as a reinforcing bio-based filler in rubber composites: A review. *Polym.-Plast. Technol. Mater.* **2023**, *62*, 54–75. [[CrossRef](#)]
11. Harussani, M.M.; Sapuan, S.M.; Nadeem, G.; Rafin, T.; Kirubaanand, W. Recent applications of carbon-based composites in defence industry: A review. *Def. Technol.* **2022**, *18*, 1281–1300. [[CrossRef](#)]
12. Huggins, T.; Wang, H.; Kearns, J.; Jenkins, P.; Ren, Z.J. Biochar as a sustainable electrode material for electricity production in microbial fuel cells. *Bioresour. Technol.* **2014**, *157*, 114–119. [[CrossRef](#)]
13. Tabac, S.; Eisenberg, D. Pyrolyze this paper: Can biomass become a source for precise carbon electrodes? *Curr. Opin. Electrochem.* **2021**, *25*, 100638. [[CrossRef](#)]
14. Snoussi, Y.; Sifaoui, I.; Khalil, A.M.; Bhakta, A.K.; Semyonov, O.; Postnikov, P.S.; Michely, L.; Pires, R.; Bastide, S.; Barroso, J.E.-P.; et al. Facile synthesis of silver decorated biochar as a novel and highly active biosourced anti-kinetoplastid agent. *Mater. Today Commun.* **2022**, *32*, 104126. [[CrossRef](#)]
15. Snoussi, Y.; Sifaoui, I.; El Garah, M.; Khalil, A.M.; Piñero, J.E.; Jouini, M.; Ammar, S.; Lorenzo-Morales, J.; Chehimi, M.M. Green, zero-waste pathway to fabricate supported nanocatalysts and anti-kinetoplastid agents from sugarcane bagasse. *Waste Manag.* **2023**, *155*, 179–191. [[CrossRef](#)]
16. Santos, J.L.; Centeno, M.A.; Odriozola, J.A. Reductant atmospheres during slow pyrolysis of cellulose: First approach to obtaining efficient char-based catalysts in one pot. *J. Anal. Appl. Pyrolysis* **2020**, *148*, 104821. [[CrossRef](#)]
17. Lee, H.W.; Lee, H.; Kim, Y.-M.; Park, R.-s.; Park, Y.-K. Recent application of biochar on the catalytic biorefinery and environmental processes. *Chin. Chem. Lett.* **2019**, *30*, 2147–2150. [[CrossRef](#)]
18. Kamran, U.; Park, S.-J. Chemically modified carbonaceous adsorbents for enhanced CO<sub>2</sub> capture: A review. *J. Clean. Prod.* **2021**, *290*, 125776. [[CrossRef](#)]
19. Lopes, R.P.; Astruc, D. Biochar as a support for nanocatalysts and other reagents: Recent advances and applications. *Coord. Chem. Rev.* **2021**, *426*, 213585. [[CrossRef](#)]
20. Luo, D.; Wang, L.; Nan, H.; Cao, Y.; Wang, H.; Kumar, T.V.; Wang, C. Phosphorus adsorption by functionalized biochar: A review. *Environ. Chem. Lett.* **2023**, *21*, 497–524. [[CrossRef](#)]
21. Goswami, L.; Kushwaha, A.; Kafle, S.R.; Kim, B.-S. Surface modification of biochar for dye removal from wastewater. *Catalysts* **2022**, *12*, 817. [[CrossRef](#)]
22. Medeiros, D.C.C.d.S.; Nzediegwu, C.; Benally, C.; Messele, S.A.; Kwak, J.-H.; Naeth, M.A.; Ok, Y.S.; Chang, S.X.; Gamal El-Din, M. Pristine and engineered biochar for the removal of contaminants co-existing in several types of industrial wastewaters: A critical review. *Sci. Total Environ.* **2022**, *809*, 151120. [[CrossRef](#)] [[PubMed](#)]
23. Tripathi, M.; Sahu, J.N.; Ganesan, P. Effect of process parameters on production of biochar from biomass waste through pyrolysis: A review. *Renew. Sustain. Energy Rev.* **2016**, *55*, 467–481. [[CrossRef](#)]
24. Tan, H.; Lee, C.T.; Ong, P.Y.; Wong, K.Y.; Bong, C.P.C.; Li, C.; Gao, Y. A Review On The Comparison Between Slow Pyrolysis And Fast Pyrolysis On The Quality Of Lignocellulosic And Lignin-Based Biochar. *IOP Conf. Ser. Mater. Sci. Eng.* **2021**, *1051*, 012075. [[CrossRef](#)]
25. Ighalo, J.O.; Iwuchukwu, F.U.; Eyankware, O.E.; Iwuozor, K.O.; Olotu, K.; Bright, O.C.; Igwegbe, C.A. Flash pyrolysis of biomass: A review of recent advances. *Clean Technol. Environ. Policy* **2022**, *24*, 2349–2363. [[CrossRef](#)]
26. Pawelczyk, E.; Wysocka, I.; Gębicki, J. Pyrolysis Combined with the Dry Reforming of Waste Plastics as a Potential Method for Resource Recovery—A Review of Process Parameters and Catalysts. *Catalysts* **2022**, *12*, 362. [[CrossRef](#)]
27. Yu, S.; Yang, X.; Zhao, P.; Li, Q.; Zhou, H.; Zhang, Y. From biomass to hydrochar: Evolution on elemental composition, morphology, and chemical structure. *J. Energy Inst.* **2022**, *101*, 194–200. [[CrossRef](#)]
28. Selvam, S.M.; Paramasivan, B. Microwave assisted carbonization and activation of biochar for energy-environment nexus: A review. *Chemosphere* **2022**, *286*, 131631. [[CrossRef](#)]
29. Jeong, S.-Y.; Lee, C.-W.; Lee, J.-U.; Ma, Y.-W.; Shin, B.-S. Laser-Induced Biochar Formation through 355 nm Pulsed Laser Irradiation of Wood, and Application to Eco-Friendly pH Sensors. *Nanomaterials* **2020**, *10*, 1904. [[CrossRef](#)]
30. You, S.; Ok, Y.S.; Chen, S.S.; Tsang, D.C.W.; Kwon, E.E.; Lee, J.; Wang, C.-H. A critical review on sustainable biochar system through gasification: Energy and environmental applications. *Bioresour. Technol.* **2017**, *246*, 242–253. [[CrossRef](#)]
31. Li, L.; Yang, M.; Lu, Q.; Zhu, W.; Ma, H.; Dai, L. Oxygen-rich biochar from torrefaction: A versatile adsorbent for water pollution control. *Bioresour. Technol.* **2019**, *294*, 122142. [[CrossRef](#)]
32. Kumar, A.; Saini, K.; Bhaskar, T. Hydrochar and biochar: Production, physicochemical properties and techno-economic analysis. *Bioresour. Technol.* **2020**, *310*, 123442. [[CrossRef](#)] [[PubMed](#)]
33. Pandey, A.; Bhaskar, T.; Stöcker, M.; Sukumaran, R. *Recent Advances in Thermochemical Conversion of Biomass*; Elsevier: Amsterdam, The Netherlands, 2015.
34. Dutta, T.; Kwon, E.; Bhattacharya, S.S.; Jeon, B.H.; Deep, A.; Uchimiya, M.; Kim, K.-H. Polycyclic aromatic hydrocarbons and volatile organic compounds in biochar and biochar-amended soil: A review. *GCB Bioenergy* **2017**, *9*, 990–1004. [[CrossRef](#)]

35. Wang, C.; Wang, Y.; Herath, H.M.S.K. Polycyclic aromatic hydrocarbons (PAHs) in biochar—Their formation, occurrence and analysis: A review. *Org. Geochem.* **2017**, *114*, 1–11. [[CrossRef](#)]
36. Bhakta, A.K.; Snoussi, Y.; Garah, M.E.; Ammar, S.; Chehimi, M.M. Brewer's Spent Grain Biochar: Grinding Method Matters. *C* **2022**, *8*, 46. [[CrossRef](#)]
37. Tang, M.; Snoussi, Y.; Bhakta, A.K.; El Garah, M.; Khalil, A.M.; Ammar, S.; Chehimi, M.M. Unusual, Hierarchically Structured Composite of Sugarcane Pulp Bagasse Biochar Loaded with Cu/Ni Bimetallic Nanoparticles for Dye Removal. *Environ. Res.* **2023**, 116232. [[CrossRef](#)]
38. Li, D.; Zhao, L.; Cao, X.; Xiao, Z.; Nan, H.; Qiu, H. Nickel-catalyzed formation of mesoporous carbon structure promoted capacitive performance of exhausted biochar. *Chem. Eng. J.* **2021**, *406*, 126856. [[CrossRef](#)]
39. Pan, X.; Gu, Z.; Chen, W.; Li, Q. Preparation of biochar and biochar composites and their application in a Fenton-like process for wastewater decontamination: A review. *Sci. Total Environ.* **2021**, *754*, 142104. [[CrossRef](#)] [[PubMed](#)]
40. Chehimi, M.M.; Pinson, J.; Mousli, F. *Aryl Diazonium Salts and Related Compounds: Surface Chemistry and Applications*; Springer Nature: London, UK, 2022.
41. Li, C.; Gao, Y.; Li, A.; Zhang, L.; Ji, G.; Zhu, K.; Wang, X.; Zhang, Y. Synergistic effects of anionic surfactants on adsorption of norfloxacin by magnetic biochar derived from furfural residue. *Environ. Pollut.* **2019**, *254*, 113005. [[CrossRef](#)]
42. Asgharzadeh, F.; Kalantary, R.R.; Gholami, M.; Jafari, A.J.; Kermani, M.; Asgharnia, H. TiO<sub>2</sub>-decorated magnetic biochar mediated heterogeneous photocatalytic degradation of tetracycline and evaluation of antibacterial activity. *Biomass Convers. Biorefin.* **2021**, 1–11. [[CrossRef](#)]
43. Wang, X.; Feng, J.; Cai, Y.; Fang, M.; Kong, M.; Alsaedi, A.; Hayat, T.; Tan, X. Porous biochar modified with polyethyleneimine (PEI) for effective enrichment of U(VI) in aqueous solution. *Sci. Total Environ.* **2020**, *708*, 134575. [[CrossRef](#)] [[PubMed](#)]
44. Detriche, S.; Bhakta, A.K.; N'Twali, P.; Delhalle, J.; Mekhalif, Z. Assessment of Catalyst Selectivity in Carbon-Nanotube Silylation. *Appl. Sci.* **2020**, *10*, 109. [[CrossRef](#)]
45. Walker, P. Silane and other adhesion promoters in adhesive technology. *Handb. Adhes. Technol.* **2003**, *2*, 205–221.
46. Lan, Y.; Wang, W. Application of tree biochar in PDMS pervaporation membranes. *Adv. Polym. Technol.* **2018**, *37*, 1979–1986. [[CrossRef](#)]
47. Zhang, M.; Zhu, H.; Xi, B.; Tian, Y.; Sun, X.; Zhang, H.; Wu, B. Surface Hydrophobic Modification of Biochar by Silane Coupling Agent KH-570. *Processes* **2022**, *10*, 301. [[CrossRef](#)]
48. Bamdad, H.; Hawboldt, K.; MacQuarrie, S. Nitrogen Functionalized Biochar as a Renewable Adsorbent for Efficient CO<sub>2</sub> Removal. *Energy Fuels* **2018**, *32*, 11742–11748. [[CrossRef](#)]
49. Moradi, P.; Hajjami, M. Stabilization of ruthenium on biochar-nickel magnetic nanoparticles as a heterogeneous, practical, selective, and reusable nanocatalyst for the Suzuki C–C coupling reaction in water. *RSC Adv.* **2022**, *12*, 13523–13534. [[CrossRef](#)]
50. Moradi, P.; Hajjami, M. Magnetization of biochar nanoparticles as a novel support for fabrication of organo nickel as a selective, reusable and magnetic nanocatalyst in organic reactions. *New J. Chem.* **2021**, *45*, 2981–2994. [[CrossRef](#)]
51. Huang, Y.; Xia, S.; Lyu, J.; Tang, J. Highly efficient removal of aqueous Hg<sup>2+</sup> and CH<sub>3</sub>Hg<sup>+</sup> by selective modification of biochar with 3-mercaptopropyltrimethoxysilane. *Chem. Eng. J.* **2019**, *360*, 1646–1655. [[CrossRef](#)]
52. Ran, W.; Zhu, H.; Shen, X.; Zhang, Y. Rheological properties of asphalt mortar with silane coupling agent modified oil sludge pyrolysis residue. *Constr. Build. Mater.* **2022**, *329*, 127057. [[CrossRef](#)]
53. Devi, G.; Nagabhooshanam, N.; Chokkalingam, M.; Sahu, S.K. EMI shielding of cobalt, red onion husk biochar and carbon short fiber-PVA composite on X and Ku band frequencies. *Polym. Compos.* **2022**, *43*, 5996–6003. [[CrossRef](#)]
54. Wu, B.; Xi, B.; He, X.; Sun, X.; Li, Q.; Ouche, Q.; Zhang, H.; Xue, C. Methane Emission Reduction Enhanced by Hydrophobic Biochar-Modified Soil Cover. *Processes* **2020**, *8*, 162. [[CrossRef](#)]
55. Qin, Y.; Xi, B.; Sun, X.; Zhang, H.; Xue, C.; Wu, B. Methane Emission Reduction and Biological Characteristics of Landfill Cover Soil Amended With Hydrophobic Biochar. *Front. Bioeng. Biotechnol.* **2022**, *10*, 905466. [[CrossRef](#)]
56. Sheng, K.; Zhang, S.; Qian, S.; Fontanillo Lopez, C.A. High-toughness PLA/Bamboo cellulose nanowhiskers bionanocomposite strengthened with silylated ultrafine bamboo-char. *Compos. Part B Eng.* **2019**, *165*, 174–182. [[CrossRef](#)]
57. Moradi, P.; Hajjami, M.; Valizadeh-Kakhki, F. Biochar as heterogeneous support for immobilization of Pd as efficient and reusable biocatalyst in C–C coupling reactions. *Appl. Organomet. Chem.* **2019**, *33*, e5205. [[CrossRef](#)]
58. Li, H.; Sun, L.; Li, W. Application of organosilanes in titanium-containing organic–inorganic hybrid coatings. *J. Mater. Sci.* **2022**, *57*, 13845–13870. [[CrossRef](#)]
59. Lu, Y.; Li, X.; Wu, C.; Xu, S. Comparison between polyether titanate and commercial coupling agents on the properties of calcium sulfate whisker/poly(vinyl chloride) composites. *J. Alloys Compd.* **2018**, *750*, 197–205. [[CrossRef](#)]
60. Elshereksi, N.W.; Ghazali, M.; Muchtar, A.; Azhari, C.H. Review of titanate coupling agents and their application for dental composite fabrication. *Dent. Mater. J.* **2017**, *36*, 539–552. [[CrossRef](#)] [[PubMed](#)]
61. Ali Sabri, B.; Meenaloshini, S.; Abreeza, N.M.; Abed, A.N. A review study on coupling agents used as ceramic fillers modifiers for dental applications. *Mater. Today Proc.* **2021**, *80*, 2315–2326. [[CrossRef](#)]
62. Zeng, Y.; Xue, Y.; Long, L.; Yan, J. Novel Crayfish Shell Biochar Nanocomposites Loaded with Ag-TiO<sub>2</sub> Nanoparticles Exhibit Robust Antibacterial Activity. *Water Air Soil Pollut.* **2019**, *230*, 50. [[CrossRef](#)]
63. Cai, K.D.; Mu, W.F. Activated carbon modified by titanate coupling agent for supercapacitor. In *Advanced Materials Research*; Trans Tech Publications Ltd.: Stafa-Zurich, Switzerland, 2012; pp. 3649–3652.

64. Li, X.; Gan, C.; Han, Z.; Yan, H.; Chen, D.; Li, W.; Li, H.; Fan, X.; Li, D.; Zhu, M. High dispersivity and excellent tribological performance of titanate coupling agent modified graphene oxide in hydraulic oil. *Carbon* **2020**, *165*, 238–250. [[CrossRef](#)]
65. Shahverdi, M.; Kouhgard, E.; Ramavandi, B. Characterization, kinetic, and isotherm data for Cr (VI) removal from aqueous solution by *Populus alba* biochar modified by a cationic surfactant. *Data Brief* **2016**, *9*, 163–168. [[CrossRef](#)]
66. Mathurasa, L.; Damrongsiri, S. Potential of using surfactants to enhance ammonium and nitrate adsorption on rice husk and its biochar. *Appl. Environ. Res.* **2017**, *39*, 11–22. [[CrossRef](#)]
67. Wiśniewska, M.; Nowicki, P.; Urban, T. Influence of surfactants with different ionic character on the structure of poly(acrylic acid) adsorption layer on the activated biocarbons surface—*Electrokinetic* and stability studies. *J. Mol. Liq.* **2021**, *332*, 115872. [[CrossRef](#)]
68. Wang, F.; Zeng, Q.; Su, W.; Zhang, M.; Hou, L.; Wang, Z.-L. Adsorption of Bisphenol A on Peanut Shell Biochars: The Effects of Surfactants. *J. Chem.* **2019**, *2019*, 2428505. [[CrossRef](#)]
69. Kosaiyakanon, C.; Kungsanant, S. Adsorption of Reactive Dyes from Wastewater Using Cationic Surfactant-modified Coffee Husk Biochar. *Environ. Nat. Resour. J.* **2019**, *18*, 21–32. [[CrossRef](#)]
70. Mi, X.; Li, G.; Zhu, W.; Liu, L. Enhanced adsorption of orange II using cationic surfactant modified biochar pyrolyzed from cornstalk. *J. Chem.* **2016**, *2016*, 8457030. [[CrossRef](#)]
71. Wiśniewska, M.; Nowicki, P. Peat-based activated carbons as adsorbents for simultaneous separation of organic molecules from mixed solution of poly(acrylic acid) polymer and sodium dodecyl sulfate surfactant. *Colloids Surf. A Physicochem. Eng. Asp.* **2020**, *585*, 124179. [[CrossRef](#)]
72. Anas, A.K.; Pratama, S.Y.; Izzah, A.; Kurniawan, M.A. Sodium Dodecylbenzene Sulfonate-Modified Biochar as An Adsorbent for The Removal of Methylene Blue. *Bull. Chem. React. Eng. Catal.* **2021**, *16*, 188–195. [[CrossRef](#)]
73. Anas, A.K.; Izzah, A.; Pratama, S.Y.; Fajarwati, F.I. Removal of methylene blue using biochar from cassava peel (*Manihot utilissima*) modified by sodium dodecyl sulphate (SDS) surfactant. *AIP Conf. Proc.* **2020**, *2229*, 030024. [[CrossRef](#)]
74. Que, W.; Jiang, L.; Wang, C.; Liu, Y.; Zeng, Z.; Wang, X.; Ning, Q.; Liu, S.; Zhang, P.; Liu, S. Influence of sodium dodecyl sulfate coating on adsorption of methylene blue by biochar from aqueous solution. *J. Environ. Sci.* **2018**, *70*, 166–174. [[CrossRef](#)]
75. He, H.; Li, W.; Deng, H.; Kang, L.; Qiu, R.; Li, X.; Liu, W.; Meng, Z. Adsorption of phenanthrene on the magnetized biochar organicoated by amphoteric modifier. *Desalination Water Treat.* **2019**, *148*, 195–201. [[CrossRef](#)]
76. Wiśniewska, M.; Nowicki, P.; Szewczuk-Karpisz, K.; Gęca, M.; Jedruchiewicz, K.; Oleszczuk, P. Simultaneous removal of toxic Pb(II) ions, poly(acrylic acid) and Triton X-100 from their mixed solution using engineered biochars obtained from horsetail herb precursor—Impact of post-activation treatment. *Sep. Purif. Technol.* **2021**, *276*, 119297. [[CrossRef](#)]
77. Hua, Z.; Wan, S.; Sun, L.; Yu, Z.; Bai, X. Role of non-ion surfactants in three-dimensional ordered porous biomass carbon foam derived from the liquefied eucalyptus sawdust for metronidazole adsorption. *J. Chem. Technol. Biotechnol.* **2018**, *93*, 3044–3055. [[CrossRef](#)]
78. Griess, P. Preliminary notice on the influence of nitrous acid on amino nitro- and amino dinitrophenol. *Annalen* **1858**, *106*, 123–125.
79. Heines, S.V. Peter Griess—Discoverer of diazo compounds. *J. Chem. Educ.* **1958**, *35*, 187. [[CrossRef](#)]
80. Mo, F.; Dong, G.; Zhang, Y.; Wang, J. Recent applications of arene diazonium salts in organic synthesis. *Org. Biomol. Chem.* **2013**, *11*, 1582–1593. [[CrossRef](#)] [[PubMed](#)]
81. Mohamed, A.A.; Salmi, Z.; Dahoumane, S.A.; Mekki, A.; Carbonnier, B.; Chehimi, M.M. Functionalization of nanomaterials with aryldiazonium salts. *Adv. Colloid Interface Sci.* **2015**, *225*, 16–36. [[CrossRef](#)]
82. Mirzaei, P.; Bastide, S.; Aghajani, A.; Bourgon, J.; Leroy, E.; Zhang, J.; Snoussi, Y.; Bensghaier, A.; Hamouma, O.; Chehimi, M.M. Bimetallic Cu–Rh Nanoparticles on Diazonium-Modified Carbon Powders for the Electrocatalytic Reduction of Nitrates. *Langmuir* **2019**, *35*, 14428–14436. [[CrossRef](#)]
83. Jawad, A.H.; Abdulhameed, A.S.; Wilson, L.D.; Syed-Hassan SS, A.; ALOthman, Z.A.; Khan, M.R. ALOthman, Mohammad Rizwan Khan. High surface area and mesoporous activated carbon from KOH-activated dragon fruit peels for methylene blue dye adsorption: Optimization and mechanism study. *Chin. J. Chem. Eng.* **2021**, *32*, 281–290. [[CrossRef](#)]
84. Abdel-Aziz, M.H.; El-Ashtouky, E.Z.; Bassyouni, M.; Al-Hossainy, A.F.; Fawzy, E.M.; Abdel-Hamid, S.M.S.; Zoromba, M.S. DFT and experimental study on adsorption of dyes on activated carbon prepared from apple leaves. *Carbon Lett.* **2021**, *31*, 863–878. [[CrossRef](#)]
85. Khalil, A.M.; Msaadi, R.; Sassi, W.; Ghanmi, I.; Pires, R.; Michely, L.; Snoussi, Y.; Chevillot-Biraud, A.; Lau-Truong, S.; Chehimi, M.M. Facile diazonium modification of pomegranate peel biochar: A stupendous derived relationship between thermal and Raman analyses. *Carbon Lett.* **2022**, *32*, 1519–1529. [[CrossRef](#)]
86. Rodd, A.L.; Creighton, M.A.; Vaslet, C.A.; Rangel-Mendez, J.R.; Hurt, R.H.; Kane, A.B. Effects of Surface-Engineered Nanoparticle-Based Dispersants for Marine Oil Spills on the Model Organism *Artemia franciscana*. *Environ. Sci. Technol.* **2014**, *48*, 6419–6427. [[CrossRef](#)] [[PubMed](#)]
87. Bensghaier, A.; Salmi, Z.; Le Droumaguet, B.; Mekki, A.; Mohamed, A.A.; Beji, M.; Chehimi, M.M. Diazonium interface chemistry and click polymerization: A novel route for carbon nanotube-polytriazole nanocomposites. *Surf. Interface Anal.* **2016**, *48*, 509–513. [[CrossRef](#)]
88. Snoussi, Y.; El Garah, M.; Khalil, A.M.; Ammar, S.; Chehimi, M.M. Immobilization of biogenic silver–copper nanoparticles over arylated biochar from sugarcane bagasse: Method and catalytic performance. *Appl. Organomet. Chem.* **2022**, *36*, e6885. [[CrossRef](#)]
89. Malins, K.; Kampars, V.; Brinks, J.; Neibolte, I.; Murnieks, R. Synthesis of activated carbon based heterogenous acid catalyst for biodiesel preparation. *Appl. Catal. B Environ.* **2015**, *176–177*, 553–558. [[CrossRef](#)]

90. Niu, S.; Ning, Y.; Lu, C.; Han, K.; Yu, H.; Zhou, Y. Esterification of oleic acid to produce biodiesel catalyzed by sulfonated activated carbon from bamboo. *Energy Convers. Manag.* **2018**, *163*, 59–65. [[CrossRef](#)]
91. Zhang, T.; Wei, H.; Gao, J.; Chen, S.; Jin, Y.; Deng, C.; Wu, S.; Xiao, H.; Li, W. Synthesis of sulfonated hierarchical carbons and their application on the production of furfural from wheat straw. *Mol. Catal.* **2022**, *517*, 112034. [[CrossRef](#)]
92. Malaika, A.; Ptaszyńska, K.; Kozłowski, M. Conversion of renewable feedstock to bio-carbons dedicated for the production of green fuel additives from glycerol. *Fuel* **2021**, *288*, 119609. [[CrossRef](#)]
93. Konwar, L.J.; Mäki-Arvela, P.; Mikkola, J.-P. SO<sub>3</sub>H-Containing Functional Carbon Materials: Synthesis, Structure, and Acid Catalysis. *Chem. Rev.* **2019**, *119*, 11576–11630. [[CrossRef](#)]
94. Zhong, Y.; Deng, Q.; Zhang, P.; Wang, J.; Wang, R.; Zeng, Z.; Deng, S. Sulfonic acid functionalized hydrophobic mesoporous biochar: Design, preparation and acid-catalytic properties. *Fuel* **2019**, *240*, 270–277. [[CrossRef](#)]
95. Wan, Z.; Sun, Y.; Tsang, D.C.W.; Khan, E.; Yip, A.C.K.; Ng, Y.H.; Rinklebe, J.; Ok, Y.S. Customised fabrication of nitrogen-doped biochar for environmental and energy applications. *Chem. Eng. J.* **2020**, *401*, 126136. [[CrossRef](#)]
96. Kaserer, N.; Kolar, P.; Hall, S.G. Nitrogen-doped biochars as adsorbents for mitigation of heavy metals and organics from water: A review. *Biochar* **2022**, *4*, 17. [[CrossRef](#)]
97. Lin, Z.; Wang, R.; Tan, S.; Zhang, K.; Yin, Q.; Zhao, Z.; Gao, P. Nitrogen-doped hydrochar prepared by biomass and nitrogen-containing wastewater for dye adsorption: Effect of nitrogen source in wastewater on the adsorption performance of hydrochar. *J. Environ. Manag.* **2023**, *334*, 117503. [[CrossRef](#)] [[PubMed](#)]
98. Chatterjee, R.; Sajjadi, B.; Chen, W.-Y.; Mattern, D.L.; Egiebor, N.O.; Hammer, N.; Raman, V. Low Frequency Ultrasound Enhanced Dual Amination of Biochar: A Nitrogen-Enriched Sorbent for CO<sub>2</sub> Capture. *Energy Fuels* **2019**, *33*, 2366–2380. [[CrossRef](#)]
99. Shahabi Nejad, M.; Sheibani, H. Super-efficient removal of arsenic and mercury ions from wastewater by nanoporous biochar-supported poly 2-aminothiophenol. *J. Environ. Chem. Eng.* **2022**, *10*, 107363. [[CrossRef](#)]
100. Thomas, R.C.; Houston, J.E.; Crooks, R.M.; Kim, T.; Michalske, T.A. Probing Adhesion Forces at the Molecular Scale. *J. Am. Chem. Soc.* **1995**, *117*, 3830–3834. [[CrossRef](#)]
101. Herath, A.; Reid, C.; Perez, F.; Pittman, C.U.; Mlsna, T.E. Biochar-supported polyaniline hybrid for aqueous chromium and nitrate adsorption. *J. Environ. Manag.* **2021**, *296*, 113186. [[CrossRef](#)]
102. Thines, K.R.; Abdullah, E.C.; Ruthiraan, M.; Mubarak, N.M.; Tripathi, M. A new route of magnetic biochar based polyaniline composites for supercapacitor electrode materials. *J. Anal. Appl. Pyrolysis* **2016**, *121*, 240–257. [[CrossRef](#)]
103. Thomas, D.; Fernandez, N.B.; Mullassery, M.D.; Surya, R. Iron oxide loaded biochar/polyaniline nanocomposite: Synthesis, characterization and electrochemical analysis. *Inorg. Chem. Commun.* **2020**, *119*, 108097. [[CrossRef](#)]
104. Ma, Y.; Zhang, T.; Zhu, P.; Cai, H.; Jin, Y.; Gao, K.; Li, J. Fabrication of Ag<sub>3</sub>PO<sub>4</sub>/polyaniline-activated biochar photocatalyst for efficient triclosan degradation process and toxicity assessment. *Sci. Total Environ.* **2022**, *821*, 153453. [[CrossRef](#)] [[PubMed](#)]
105. Ma, Y.; Liu, W.-J.; Zhang, N.; Li, Y.-S.; Jiang, H.; Sheng, G.-P. Polyethylenimine modified biochar adsorbent for hexavalent chromium removal from the aqueous solution. *Bioresour. Technol.* **2014**, *169*, 403–408. [[CrossRef](#)]
106. Qu, J.; Zhang, X.; Bi, F.; Wang, S.; Zhang, X.; Tao, Y.; Wang, Y.; Jiang, Z.; Zhang, Y. Polyethylenimine-grafted nitrogen-doping magnetic biochar for efficient Cr(VI) decontamination: Insights into synthesis and adsorption mechanisms. *Environ. Pollut.* **2022**, *313*, 120103. [[CrossRef](#)] [[PubMed](#)]
107. Geça, M.; Wiśniewska, M.; Nowicki, P. Simultaneous Removal of Polymers with Different Ionic Character from Their Mixed Solutions Using Herb-Based Biochars and Activated Carbons. *Molecules* **2022**, *27*, 7557. [[CrossRef](#)] [[PubMed](#)]
108. Parameswari, E.; Kalaiarasi, R.; Davamani, V.; Ilakiya, T.; Kalaiselvi, P.; Sebastian, S.P. Utility of Surface-Modified Biochar for Sequestration of Heavy Metals in Water. In *Biochar and Its Application in Bioremediation*; Thapar Kapoor, R., Treichel, H., Shah, M.P., Eds.; Springer Nature Singapore: Singapore, 2021.
109. Tian, H.; Huang, C.; Wang, P.; Wei, J.; Li, X.; Zhang, R.; Ling, D.; Feng, C.; Liu, H.; Wang, M.; et al. Enhanced elimination of Cr(VI) from aqueous media by polyethyleneimine modified corn straw biochar supported sulfide nanoscale zero valent iron: Performance and mechanism. *Bioresour. Technol.* **2023**, *369*, 128452. [[CrossRef](#)]
110. Jiang, Q.; Xie, W.; Han, S.; Wang, Y.; Zhang, Y. Enhanced adsorption of Pb(II) onto modified hydrochar by polyethyleneimine or H<sub>3</sub>PO<sub>4</sub>: An analysis of surface property and interface mechanism. *Colloids Surf. A Physicochem. Eng. Asp.* **2019**, *583*, 123962. [[CrossRef](#)]
111. Xiao, Z.; Xie, Y.; Militz, H.; Mai, C. Effect of glutaraldehyde on water related properties of solid wood. *Holzforschung* **2010**, *64*, 483–488. [[CrossRef](#)]
112. Pandey, D.; Daverey, A.; Dutta, K.; Arunachalam, K. Enhanced adsorption of Congo red dye onto polyethyleneimine-impregnated biochar derived from pine needles. *Environ. Monit. Assess.* **2022**, *194*, 880. [[CrossRef](#)]
113. Mao, W.; Zhang, Y.; Luo, J.; Chen, L.; Guan, Y. Novel co-polymerization of polypyrrole/polyaniline on ferrate modified biochar composites for the efficient adsorption of hexavalent chromium in water. *Chemosphere* **2022**, *303*, 135254. [[CrossRef](#)]
114. dos Reis, G.S.; Bergna, D.; Grimm, A.; Lima, E.C.; Hu, T.; Naushad, M.; Lassi, U. Preparation of highly porous nitrogen-doped biochar derived from birch tree wastes with superior dye removal performance. *Colloids Surf. A Physicochem. Eng. Asp.* **2023**, *669*, 131493. [[CrossRef](#)]
115. Wang, W.; Chen, M. Catalytic degradation of sulfamethoxazole by peroxymonosulfate activation system composed of nitrogen-doped biochar from pomelo peel: Important roles of defects and nitrogen, and detoxification of intermediates. *J. Colloid Interface Sci.* **2022**, *613*, 57–70. [[CrossRef](#)]

116. Yu, B.; Man, Y.; Wang, P.; Wu, C.; Xie, J.; Wang, W.; Jiang, H.; Zhang, L.; Zhang, Y.; Mao, L.; et al. Catalytic degradation of dimethomorph by nitrogen-doped rice husk biochar. *Ecotoxicol. Environ. Saf.* **2023**, *257*, 114908. [[CrossRef](#)]
117. Cheng, T.; Bian, Y.; Li, J.; Ma, X.; Yang, L.; Zhou, L.; Wu, H. Nitrogen-doped porous biochar for selective adsorption of toluene under humid conditions. *Fuel* **2023**, *334*, 126452. [[CrossRef](#)]
118. Gao, G.; Hu, X.; Wang, Q.; Li, C.; Chen, Q.; Zhang, L.; Gao, W.; Ding, K.; Huang, Y.; Zhang, S. Functionalization of the biochar from melon seed shell via introducing nitrogen species. *J. Environ. Chem. Eng.* **2023**, *11*, 109781. [[CrossRef](#)]
119. Zhang, Y.; Deng, J.; Liu, Y.; Li, H.; Tan, M.; Qin, X.; Wu, Z.; Huang, Z.; Li, X.; Lu, Q. Co-adsorption of tetracycline and Cu(II) onto a novel amino-functionalized biochar: Adsorption behavior and mechanism. *Environ. Sci. Water Res. Technol.* **2023**, *9*, 1577–1586. [[CrossRef](#)]
120. Geng, Y.; Du, Y.; Guo, T.; Zhang, Y.; Bedane, A.H.; Ren, P. Isothermal and isovolumetric process of CO<sub>2</sub> adsorption on nitrogen-doped biochar: Equilibrium and non-equilibrium states. *Case Stud. Therm. Eng.* **2023**, *44*, 102814. [[CrossRef](#)]
121. Yue, L.; Xia, Q.; Wang, L.; Wang, L.; DaCosta, H.; Yang, J.; Hu, X. CO<sub>2</sub> adsorption at nitrogen-doped carbons prepared by K<sub>2</sub>CO<sub>3</sub> activation of urea-modified coconut shell. *J. Colloid Interface Sci.* **2018**, *511*, 259–267. [[CrossRef](#)]
122. Zhao, W.; Liu, S.; Yin, M.; He, Z.; Bi, D. Co-pyrolysis of cellulose with urea and chitosan to produce nitrogen-containing compounds and nitrogen-doped biochar: Product distribution characteristics and reaction path analysis. *J. Anal. Appl. Pyrolysis* **2023**, *169*, 105795. [[CrossRef](#)]
123. Khalil, A.M.; Michely, L.; Pires, R.; Bastide, S.; Jlassi, K.; Ammar, S.; Jaziri, M.; Chehimi, M.M. Copper/nickel-decorated olive pit biochar: One pot solid state synthesis for environmental remediation. *Appl. Sci.* **2021**, *11*, 8513. [[CrossRef](#)]
124. Boubkr, L.; Bhakta, A.K.; Snoussi, Y.; Moreira Da Silva, C.; Michely, L.; Jouini, M.; Ammar, S.; Chehimi, M.M. Highly Active Ag-Cu Nanocrystal Catalyst-Coated Brewer's Spent Grain Biochar for the Mineralization of Methyl Orange and Methylene Blue Dye Mixture. *Catalysts* **2022**, *12*, 1475.
125. Zhao, J.; Chen, T.; Hou, C.; Huang, B.; Du, J.; Liu, N.; Zhou, X.; Zhang, Y. Efficient Activation of Peroxymonosulfate by Biochar-Loaded Zero-Valent Copper for Enrofloxacin Degradation: Singlet Oxygen-Dominated Oxidation Process. *Nanomaterials* **2022**, *12*, 2842. [[CrossRef](#)]
126. He, S.; Wu, L.; Zeng, Y.; Jia, B.; Liang, L. Preparation of Ce-Ag bimetallic modified biochar composite for the efficient removal of sulfathiazole and its mechanism. *Mater. Today Commun.* **2022**, *33*, 104577. [[CrossRef](#)]
127. Yu, F.; Tian, F.; Zou, H.; Ye, Z.; Peng, C.; Huang, J.; Zheng, Y.; Zhang, Y.; Yang, Y.; Wei, X.; et al. ZnO/biochar nanocomposites via solvent free ball milling for enhanced adsorption and photocatalytic degradation of methylene blue. *J. Hazard. Mater.* **2021**, *415*, 125511. [[CrossRef](#)]
128. Omiri, J.; Snoussi, Y.; Bhakta, A.K.; Truong, S.; Ammar, S.; Khalil, A.M.; Jouini, M.; Chehimi, M.M. Citric-Acid-Assisted Preparation of Biochar Loaded with Copper/Nickel Bimetallic Nanoparticles for Dye Degradation. *Colloids Interfaces* **2022**, *6*, 18. [[CrossRef](#)]
129. Fan, J.; Cai, C.; Chi, H.; Reid, B.J.; Coulon, F.; Zhang, Y.; Hou, Y. Remediation of cadmium and lead polluted soil using thiol-modified biochar. *J. Hazard. Mater.* **2020**, *388*, 122037. [[CrossRef](#)]
130. Saremi, F.; Miroliaei, M.R.; Shahabi Nejad, M.; Sheibani, H. Adsorption of tetracycline antibiotic from aqueous solutions onto vitamin B6-upgraded biochar derived from date palm leaves. *J. Mol. Liq.* **2020**, *318*, 114126. [[CrossRef](#)]
131. Ayedi, N.; Rzig, B.; Bellakhal, N. Catalytic Hydrothermal Carbonization of Olive Wood Charcoal for Methylene Blue Adsorption from Wastewater: Optimization, Isotherm, Kinetic and Thermodynamic Studies. *Chem. Afr.* **2023**, *6*, 765–778. [[CrossRef](#)]
132. Alharbi, H.A.; Hameed, B.H.; Alotaibi, K.D.; Al-Oud, S.S.; Al-Modaihsh, A.S. Recent methods in the production of activated carbon from date palm residues for the adsorption of textile dyes: A review. *Front. Environ. Sci.* **2022**, *10*, 996953. [[CrossRef](#)]
133. Jlassi, K.; Mallick, S.; Eribi, A.; Chehimi, M.M.; Ahmad, Z.; Touati, F.; Krupa, I. Facile preparation of NS co-doped graphene quantum dots (GQDs) from graphite waste for efficient humidity sensing. *Sens. Actuators B Chem.* **2021**, *328*, 129058. [[CrossRef](#)]

**Disclaimer/Publisher's Note:** The statements, opinions and data contained in all publications are solely those of the individual author(s) and contributor(s) and not of MDPI and/or the editor(s). MDPI and/or the editor(s) disclaim responsibility for any injury to people or property resulting from any ideas, methods, instructions or products referred to in the content.